Review

Analysis and Risks of Emerging Contaminants and Microplastics in Natural and Treated Waters and Human Health: A Critical Review

Maryam Mallek * and Damià Barceló

Posted Date: 7 April 2026

doi: 10.20944/preprints202604.0384.v1

Keywords: emerging contaminants; microplastics; high-resolution mass spectrometry; suspect screening; non-target screening; water monitoring; risk assessment

 doi:10.20944/preprints202604.0384.v1

Review

Analysis and Risks of Emerging Contaminants and Microplastics in Natural and Treated Waters and Human Health: A Critical Review

Maryam Mallek [1,2,*] and Damià Barceló [3]

[1] Laboratory of Material Sciences and Environment, Faculty of Sciences, University of Sfax, Route de la Soukra Km 3.5, BP 1171, Sfax 3000, Tunisia
[2] Department de Química, Facultat de Ciències, Universitat de Girona, C/Mª Aurèlia Capmany, 69,17003 Girona, Spain
[3] Chemistry and Physics Department, University of Almeria, Ctra Sacramento s/n, 04120, Almería, Spain
* Correspondence: mallek.mariem87@gmail.com

Abstract

Emerging contaminants (ECs) and microplastics (MPs) are increasingly detected in surface waters, wastewaters, and drinking water, often as complex mixtures, transformation products, and particle-associated burdens that challenge routine monitoring. This critical review examines current analytical strategies for the detection and characterization of both molecular and particulate emerging contaminants in aquatic systems, with particular emphasis on their relevance to environmental and human-health risk assessment. For molecular ECs, targeted LC–MS/MS and GC–MS(/MS) approaches are evaluated alongside high-resolution mass spectrometry (HRMS)-based suspect and non-target screening, retrospective data mining, and transformation-product elucidation. For MPs, particle-resolved vibrational spectroscopy (μ-FTIR and μ-Raman) is critically assessed in comparison with complementary thermal/mass-based methods such as pyrolysis–GC–MS and TED–GC–MS. Particular attention is given to the influence of sampling design, matrix-adapted sample preparation, analytical confidence, and method-dependent size and polymer coverage on data quality and interstudy comparability. The review further highlights the risks of ECs in relation to exposure pathways, mixture effects, and the role of MPs as vectors of ECs, additives, and microorganisms. Finally, key priorities are identified for next-generation monitoring frameworks, including harmonized workflows, transparent confidence reporting, and stronger integration of analytical evidence with fate, exposure, and risk assessment.

Keywords: emerging contaminants; microplastics; high-resolution mass spectrometry; suspect screening; non-target screening; water monitoring; risk assessment

1. Introduction

The occurrence of emerging contaminants (ECs) and microplastics (MPs) in aquatic environments has become a major challenge for environmental analytical chemistry thanks to their expanding diversity, widespread detection, and potential relevance for ecosystem and human health [1,2]. This challenge is further intensified by water scarcity, wastewater reclamation, and water reuse practices, which increase opportunities for contaminant recirculation across water, soil, crops, food, and biota [3].

ECs comprise a chemically and biologically diverse group of substances, including pharmaceuticals and personal care products, per- and polyfluoroalkyl substances (PFAS), disinfection by-products (DBPs), endocrine-disrupting chemicals, pesticides, algal toxins, nanomaterials, tire-derived chemicals, and antibiotic resistance genes (ARGs) [4–13]. In parallel, MPs

 doi:10.20944/preprints202604.0384.v1

have emerged as ubiquitous particulate contaminants in surface waters, wastewaters, and drinking water systems, raising concern not only because of their physical presence, but also because of their interactions with additives, sorbed pollutants, metals, and microorganisms [14]. Their environmental relevance is further underscored by large-scale plastic pollution estimates, indicating that between 307 and 925 million litter items are released annually from Europe into the ocean, with fragments and single-use plastics accounting for the majority of the observed debris [15].

Conventional wastewater and drinking water treatment processes were not originally designed to remove many of these contaminants, which contributes to their continued release into receiving waters and, in some cases, their entry into drinking water supplies [11–13]. As a result, ECs and MPs are frequently detected at trace and ultra-trace levels, often as complex mixtures that complicate both analytical determination and risk assessment [14,15]. In urban receiving waters, this challenge is amplified by short-lived episodic inputs; for example, 6PPD-quinone (6PPDQ) has been reported at concentrations up to 2.3 μg L^{-1} during stormflow events and remained above 2 μg L^{-1} for more than 10 h, highlighting the limitations of single grab samples for capturing peak exposure conditions [16]. For MPs, environmental concern is further reinforced by projections that plastic inputs to soils may increase from 34–55 million tons in 2019 to 260 million tons, while sewage sludge reuse, wastewater irrigation, biosolids, composting, and fragmentation of mulching films and other plastic wastes are recognized as major sources of MPs in agroecosystems [17]. These concerns are combined by the formation of transformation products during treatment and environmental processes, particularly for pharmaceuticals, pesticides, PFAS precursors, and DBPs, some of which may persist, evade routine monitoring, and exhibit toxicity comparable to or greater than that of their parent compounds [12,18–20].

From an analytical perspective, molecular and particulate emerging contaminants present distinct but complementary challenges. Molecular ECs require highly sensitive and selective techniques capable of detecting a broad range of compounds at ng L^{-1} or lower concentrations in complex aqueous matrices [21]. Targeted analysis based on liquid chromatography–tandem mass spectrometry (LC–MS/MS) and gas chromatography–tandem mass spectrometry (GC–MS/MS) remains the reference approach for the quantitative determination of priority contaminants; however, these methods are inherently restricted to predefined analytes and therefore cannot fully address the continuously evolving chemical space of emerging pollutants [22,23]. In contrast, high-resolution mass spectrometry (HRMS) has substantially expanded analytical capabilities through suspect and non-target screening, enabling the detection, structural annotation, and retrospective interrogation of known, unknown, and newly recognized contaminants, including transformation products, novel PFAS, and rubber-derived chemicals [24–27]. This is especially relevant for PFAS, whose extreme persistence is closely linked to the high strength of the C–F bond, contributing to their resistance to both environmental and treatment-induced degradation [28].

MPs, however, are particulate emerging contaminants whose analysis relies on fundamentally different methodological principles. Their characterization requires information on particle size, shape, and polymer composition, which is commonly obtained using spectroscopic techniques such as μ-FTIR and Raman microscopy, or complementary thermal analytical methods such as pyrolysis–GC/MS and thermal extraction–desorption GC/MS [29]. Nevertheless, current workflows remain method-dependent and incomplete, as no single analytical technique can yet provide comprehensive characterization across all environmentally relevant particle-size classes and matrix types. Interlaboratory studies have further highlighted harmonization as a major unmet need. Current recommendations emphasize standardized reporting units, consistent classification of particle forms, explicit reporting of minimum detectable size and instrumental detection limits, polymer confirmation by appropriate spectroscopic or thermal techniques, and detailed quality assurance/quality control (QA/QC) documentation [30]. Despite substantial progress, insufficient harmonization, limitations in size detectability, and persistent challenges related to contamination control continue to hamper comparability across studies, particularly for small MPs and nanoplastics [31]. In addition, apparent “removal” from water often reflects transfer to solids rather than true

 doi:10.20944/preprints202604.0384.v1

elimination, underscoring the need for robust and comparable analytical strategies across both aqueous and solid compartments [32].

Beyond analytical detection, increasing attention is being paid to the environmental and human health implications of ECs and MPs. Chronic exposure to low concentrations of EC mixtures, including endocrine disruptors, PFAS, pesticides, and pharmaceutical residues, raises concerns about endocrine disruption, antimicrobial resistance, and long-term toxicity [5,6,10,33]. For MPs, potential risks arise from their physical presence, associated chemical additives, and their capacity to act as vectors for organic contaminants, metals, and microorganisms, including resistance determinants [34–36]. Under water reuse and food production scenarios, these concerns may extend beyond aquatic exposure alone to include transfer through soil–plant systems, trophic pathways, and ultimately human dietary exposure [34,37,38]. Nevertheless, risk assessment remains strongly constrained by analytical uncertainties, incomplete chemical characterization, and limited toxicological evidence, underscoring the need for more integrated analytical-toxicological frameworks.

In this context, the present review critically evaluates current analytical strategies for the determination of molecular and particulate ECs in natural and treated waters. Particular emphasis is placed on how recent analytical advances especially HRMS, suspect and non-target screening strategies, and complementary particle-resolved approaches for MPs that can improve the reliability of occurrence assessment and strengthen the integration of monitoring data with environmental and human-health risk evaluation. Sampling and sample preparation strategies, targeted and non-target analytical methods, and emerging directions such as retrospective data mining and transformation-product analysis are examined. By identifying current limitations, methodological gaps, and future analytical priorities, this review aims to support the development of harmonized, robust, and risk-relevant frameworks for the monitoring and assessment of ECs and MPs in aquatic systems.

2. Occurrence and Sources of Emerging Contaminants and Microplastics in Water Systems

2.1. Molecular Emerging Contaminants

Molecular emerging contaminants occur in water systems through interconnected source pathways that include landfills, WWTPs, agricultural reuse practices, urban runoff, consumer products, industrial emissions, and long-range atmospheric transport. Their occurrence is shaped not only by input intensity, but also by hydrology, partitioning behavior, transformation, and incomplete removal during treatment. As a result, aquatic environments receive complex mixtures of antibiotics, pharmaceuticals and PPCPs, PFAS, tire-derived chemicals, cyanotoxins, nanomaterials, and resistance-related contaminants across concentration ranges extending from ng L^{-1} to μg L^{-1} and, in concentrated matrices such as landfill leachates, even mg L^{-1} levels [37,39].

Landfills are increasingly recognized as important reservoirs of both biological and chemical emerging contaminants. Metagenomic analysis of municipal solid-waste landfill refuse revealed diverse ARG profiles, with multidrug resistance genes accounting for 39.78% of total ARG abundance and showing strong associations with mobile genetic elements and heavy metals, consistent with co-selection processes [40]. This biological role is paralleled by their chemical burden: a global synthesis identified 172 PPCPs in landfill leachates, often at concentrations exceeding those reported in municipal wastewater and, in some cases, reaching the mg L^{-1} range [41]. Among the most frequently detected compounds, DEET reached a maximum of 52.8 mg L^{-1} [42]. Landfill leachates are also hydrologically dynamic, with wet-season mean total PPCP concentrations of 17.0 μg L^{-1} compared with 3.8 μg L^{-1} in drier months, and individual compounds ranging from <LOQ to 586 μg L^{-1} [43]. Compared with WWTP effluents, landfills therefore represent less controlled but often more concentrated reservoirs capable of releasing both resistance determinants and high contaminant loads to surrounding waters.

 doi:10.20944/preprints202604.0384.v1

WWTPs, however, are more continuous but still incomplete barriers, acting simultaneously as point sources and redistribution nodes. At the global scale, domestic human antibiotic consumption was estimated at 30,300 tons yr^{-1}, of which 9500 tons (31%) enter rivers and 3250 tons (11%) reach oceans or inland sinks [44]. Under low-flow conditions, approximately 6 million km of rivers may exceed thresholds relevant to ecosystem protection and/or resistance promotion, with amoxicillin, ceftriaxone, and cefixime identified as dominant contributors. At the treatment scale, realistic pharmaceutical mixtures can intensify such pressure: diclofenac (50 μg L^{-1}), metformin (26 μg L^{-1}), and 17β-estradiol (24.8 μg L^{-1}) lowered ciprofloxacin LOECs from 3.7 to 0.12 μg L^{-1}, from 0.98 to 0.24 μg L^{-1}, and from 1.95 to 0.24 μg L^{-1}, respectively [33]. In parallel, about 80% of PPCPs may partition into primary and waste activated sludge, where concentrations can reach 4500 ng g^{-1} dw for ciprofloxacin, 2190 ng g^{-1} for norfloxacin, 13,000 ng g^{-1} for triclosan, and 1360 ng g^{-1} for triclocarban [45,46]. Strong partitioning into solids is also reflected by solid–water distribution coefficients such as log Kd ≈ 3.5 for triclosan [47]. During anaerobic digestion, many PPCPs inhibit methane production, with reductions of 50.4% for erythromycin and 62.2% for carbamazepine [48,49]. Thus, compared with landfill leachates, sludge represents a more concentrated but less mobile reservoir, although land application and digestate reuse create secondary release pathways to soils and waters.

Agricultural reuse practices extend this contamination into the soil–water–plant continuum. In intensive greenhouse systems, polyethylene mulching films harbored 295 ARGs spanning 11 resistance classes, while irrigation water contained clarithromycin at 4.2 μg L^{-1}, ofloxacin at 0.7 μg L^{-1}, and trimethoprim at 0.8 μg L^{-1}, indicating sustained selective pressure at soil–water interfaces [36]. Similarly, treated wastewater and biosolids introduce pharmaceuticals, antibiotics, β-blockers, lipid regulators, and synthetic musks into soils and crops, with documented uptake of more than 100 PPCPs under field and greenhouse conditions [37]. Although concentrations in agro-food systems are generally lower than those in landfill leachates, they are more directly relevant to dietary exposure. For example, in tomatoes irrigated with treated wastewater, only carbamazepine was detected above LOQ in fruits under non-spiked conditions (22 ng g^{-1}), whereas spiked irrigation water (1 mg L^{-1}) produced detectable fruit concentrations of several compounds and up to 17 CECs distributed as roots > leaves > stems, indicating strong root retention and limited translocation to edible tissues [38]. Controlled greenhouse experiments further showed that pore water is a better predictor of pharmaceutical accumulation than bulk soil concentration: in radish grown in soils spiked at 283–504 ng g^{-1}, 14 of 15 pharmaceuticals accumulated in tissues, whereas porewater-based factors varied much less than soil-based values [50]. Together, these results indicate that occurrence assessment under reuse scenarios should integrate water, soil, and porewater compartments rather than bulk soil concentrations alone. In Baix Llobregat Agrarian Park (Catalonia), which includes more than 3400 ha partially irrigated with treated wastewater, over 100 chemical entities were detected at the irrigation-water abstraction point, highlighting the limited design of many WWTPs for micropollutant removal and the potential for accumulation in amended soils. The same review also reported the scale of land application as a pathway, with more than 3 million tons yr^{-1} of biosolids recycled to agricultural land in the UK. Besides, it emphasized that biosolids can introduce both legacy and emerging contaminants, including PCBs/dioxins, PPCPs, plastics, and PFAS, which are still incompletely addressed in reuse policy framework [51].

Within the broader PPCP group, personal care products represent a particularly persistent diffuse source because high formulation allowances support continuous consumer-driven emissions. Under EU Regulation 1223/2009/EC, several UV filters are permitted at percent-level concentrations, including benzophenone-3 (10%), benzophenone-4 (5%), 4-methylbenzylidene camphor (4%), ethylhexyl methoxycinnamate (10%), octocrylene (10%), ethylhexyl dimethyl PABA (8%), ethylhexyl salicylate (5%), and homosalate (10%), while phenoxyethanol is permitted at up to 1% and parabens up to 0.4% for a single ester and 0.8% for mixtures [52]. These large upstream use reservoirs help explain sustained emissions to wastewater and solid-waste streams. Many PCP ingredients are also strongly hydrophobic; several UV filters show log Kow values of about 4–8, and 4-methylbenzylidene camphor exhibited a bioaccumulation factor of 9700–23,000 in roach. Artificial sweeteners provide a

 doi:10.20944/preprints202604.0384.v1

complementary example of persistent wastewater-linked occurrence: in Victoria Harbor, acesulfame reached 0.22 mg L^{-1} in summer, while saccharin and cyclamate reached 0.11 and 0.10 mg L^{-1} in winter [52]. These sub-mg L^{-1} concentrations are markedly higher than the ng L^{-1}–μg L^{-1} levels commonly reported for many PPCPs in surface waters, indicating that consumer-derived compounds can contribute substantially to dissolved contaminant burdens [53].

Beyond direct emission sources, remote and high-altitude ecosystems are increasingly recognized as reservoirs of persistent and emerging contaminants. High-mountain Alpine lakes act as "cold traps" for POPs and selected contaminants of emerging concern, including PCBs, DDTs, PBDEs, PAHs, synthetic musks, PFAS and MPs. Despite minimal local anthropogenic activity, atmospheric transport, glacial meltwater remobilization, and seasonal deposition promote accumulation in sediments and biota. Among the reviewed studies, sediments were the dominant matrix (≈65%), followed by fish (≈33%), whereas water was rarely investigated (≈2%), which is consistent with the strong partitioning of hydrophobic contaminants [54]. Sediment-core records further revealed secondary concentration increases associated with glacier retreat, indicating cryospheric re-release of stored pollutants. In the same context, aerosol-bound C_{60} and C_{70} were detected in 43 Mediterranean marine-air samples, with median concentrations of 0.06 and 0.48 ng m^{-3}, respectively, and a maximum C_{70} concentration of 233.8 ng m^{-3}, showing that engineered nanomaterials, like legacy contaminants, can also undergo long-range atmospheric dispersal [55].

Long-range transport and climate forcing are likewise reflected in biological and bloom-mediated exposure pathways. In polar bears from Western and Southern Hudson Bay, 109 PCA homologues spanning C8–C26 were detected, with ΣPCA concentrations up to 260 ng g^{-1} lipid. However, temporal trends diverged between subpopulations, suggesting that contaminant burdens are modulated not only by atmospheric transport but also by climate-driven dietary shifts [56]. Cyanotoxins represent a different but equally climate-sensitive occurrence pattern: under eutrophic and thermally stable conditions, microcystin concentrations frequently exceed the WHO provisional drinking-water guideline of 1 μg L^{-1}, and multiple toxin families, including microcystins (MCs), cylindrospermopsin (CYN), anatoxin-a (ATX), and nodularin (NOD), often co-occur in bloom-impacted waters [56,57]. Thus, compared with remote contaminant accumulation driven by deposition and remobilization, cyanotoxin occurrence reflects in situ production enhanced by changing environmental conditions.

In contrast to these diffuse and climate-mediated pathways, urban runoff is a direct and quantitatively important source of tire-wear-derived contaminants. In multi-site U.S. monitoring, 6PPD-quinone (6PPDQ) ranged from ~1.3 ng L^{-1} to 75 μg L^{-1} in roadway runoff, while benzothiazole-2-sulfonic acid reached ~40–50 μg L^{-1} and additional tire-related transformation products occurred at ~0.5–2 μg L^{-1} [58,59]. These data show that traffic-derived ECs span concentrations from ng L^{-1} to tens of μg L^{-1} and commonly occur as parent–transformation product mixtures [60]. Unlike remote systems, where inputs are diffuse and delayed, tire-derived contaminants display strong pulse-like behavior linked to rainfall and surface runoff.

Nonetheless, runoff is not the only relevant pathway for tire-derived chemicals. Recycled rubber materials contained 6PPD, DPPD, and DTPD in all tested samples, at concentrations 0.5–6 times higher than those of other monitored rubber additives [61], while benzothiazoles in crumb rubber reached 171 ppm for BT and 80.9 ppm for HOBT, with about 50% of total content being water-leachable [62]. Riverine monitoring in the Pearl River Delta reported dissolved benzothiazoles at 220–611 ng L^{-1}, with annual export of 79 tons yr^{-1} for Σbenzothiazoles [63], and seawater-to-atmosphere transfer was also confirmed by aerosol concentrations of 13 ng m^{-3} and gas-phase levels up to 53 ppt [64]. Compared with storm-driven roadway runoff, these studies indicate more sustained watershed-scale and marine-atmospheric transport of tire-derived additives.

Continuous urban and industrial releases further reinforce this source category. In four Hong Kong WWTPs, influent ΣPPD-Qs ranged from 14 to 830 ng L^{-1} and effluent concentrations remained measurable at 2.8–140 ng L^{-1} after partial removal [23]. Rubber manufacturing represents an even more concentrated source, with median levels of 114 μg g^{-1} for ΣPPDs and 354 μg g^{-1} for ΣPPD-Qs

 doi:10.20944/preprints202604.0384.v1

in tire-factory workshop dust [65]. Thus, compared with episodic runoff, wastewater effluents and manufacturing emissions represent more continuous release pathways, together demonstrating that tire-derived molecular ECs arise from overlapping urban, industrial, and legacy sources.

The environmental relevance of these compounds is reinforced by both analytical detectability and toxicological potency. Current methods achieve sub-ng L^{-1} sensitivity in water, with 6PPDQ MDLs below 0.1 ng L^{-1}, while $PM_{2.5}$ LODs reach 0.07 pg m^{-3} for 6PPD and 0.02 pg m^{-3} for 6PPDQ [66]. At the same time, 6PPDQ has an aqueous solubility of 38 ± 10 μg L^{-1}, about 900 times higher than the acute LC_{50} for coho salmon (95 ng L^{-1}), and reported fish LC_{50} values range from <0.10 to 500 μg L^{-1} depending on species [67–69]. A multi-year storm-event study further showed 6PPDQ peaks of 33–160 ng L^{-1} and event-scale exports up to 2.7 g per storm [70]. Compared with many other urban ECs, these data indicate an especially close overlap between environmental occurrence, analytical detectability, and biological effect thresholds.

In addition to roadway runoff, legacy disposal of whole tires represents an overlooked but persistent source of tire-derived chemicals. The Investigation of an underwater tire dump in Hjelmås Bay (Norway), where tires had remained submerged for more than 50 years, revealed elevated sediment concentrations of Zn, Pb, and Cu near the dump center, with Zn as the dominant metal [13]. Bis(2-ethylhexyl) phthalate (DEHP) was the predominant phthalate in sediments, while non-target LC–HRMS screening of overlying waters identified 20 features potentially linked to tire degradation, including N,N′-diphenylguanidine (DPG). Unlike storm-driven urban pulses, these results indicate that submerged whole tires can act as long-term marine reservoirs of trace metals and additive-derived compounds.

Engineered metal and metal oxide nanoparticles further broaden the spectrum of molecular emerging contaminants in urbanized watersheds. Using single-particle ICP–MS, Ti-, Ce-, and Ag-bearing nanoparticles were quantified in the Besòs and Ebro river basins and adjacent Mediterranean coastal waters. Ti-NPs and Ce-NPs were ubiquitous, with concentrations of 23.2 × 10^6–298 × 10^6 and 18.1 × 10^6–278 × 10^6 particles L^{-1}, respectively, largely reflecting natural mineral backgrounds such as monazite-derived Ce. In contrast, Ag-NPs occurred at 17.9 × 10^6–45.1 × 10^6 L^{-1} and were mainly associated with hotspots downstream of WWTP discharges, indicating a more localized anthropogenic signature [39]. Coastal concentrations were substantially attenuated by river–sea dilution, although occasional offshore detection of Ce-NPs suggested combined fluvial and atmospheric inputs. Compared with dissolved molecular contaminants, engineered nanoparticles therefore require particle-resolved monitoring to distinguish anthropogenic particles from natural colloids.

The interpretation of nanoparticle occurrence is further complicated by transformation during wastewater treatment. In model WWTP effluents, silver nanoparticles underwent complete sulfidation to Ag_2S, whereas TiO_2 nanoparticles (anatase/rutile ≈ 80/20) showed no detectable structural transformation [71]. Full-scale pilot evidence similarly showed that, over 60 weeks, PVP-coated AgNPs were converted to Ag_2S regardless of whether Ag entered as nanoparticles or dissolved ions, while ZnO nanoparticles were transformed to ZnS, $Zn_3(PO_4)_2$, and Zn associated with Fe oxy/hydroxides [72]. Together, these studies indicate that WWTP processes can substantially reshape nanomaterial speciation and promote convergence toward geochemically stable phases. However, in contrast to simple removal-based interpretations, such transformation does not necessarily imply complete risk elimination, since altered speciation may still permit long-term persistence and bioavailability [71,72].

Field and mesocosm studies have proven that nanoparticle transformation does not necessarily prevent long-term bioavailability. In freshwater wetland systems exposed to Ag^0, Ag_2S, CuO, and CuS nanoparticles (3 g total metal), both pristine and sulfidized forms exhibited similar partitioning between surficial sediments and Egeria densa, with ~50% of added metal associated with plant tissues after 9 months [73]. Likewise, in an 18-month emergent wetland study, PVP-coated AgNPs accumulated mainly in soils and sediments (~70 wt% of added Ag) and were substantially transformed into Ag_2S (≈52–55%), yet Ag burdens of 0.5–3.3 μg g^{-1} wet weight were still detected in

 doi:10.20944/preprints202604.0384.v1

fish and invertebrates [74]. Together, these findings indicate that aging alters speciation but does not eliminate biological uptake or trophic transfer.

Consumer products also represent important upstream sources of engineered TiO_2 to wastewater. In washing experiments, five UV-protection textiles released only 0.01–0.06 wt% of total Ti per wash, whereas one antimicrobial textile released ~5 mg L^{-1} Ti (3.4 wt%) [75]. Commercial products contained Ti from <0.01 μg mg^{-1} in shampoos and deodorants to 1–10 wt% in toothpastes and sunscreens, while food-grade TiO_2 (E171) showed a broad size distribution of 30–400 nm, with ~36% of particles <100 nm [76]. A field study further confirmed the release of sunscreen-derived TiO_2 into recreational waters using SEM, Ti/Al ratios, and sp-ICP-MS [77]. These results emphasize that environmentally relevant TiO_2 inputs originate from multiple consumer pathways and may differ structurally from model nanomaterials used in fate studies.

For PFAS, total-fluorine approaches continue to show that target monitoring substantially underestimates environmental fluorinated burdens. In wastewater, recoveries for 11 standards ranged from 61% to 105%, whereas bulk total organic halogen analysis indicated >98% more organically bound halogen than captured by target PFAS analysis alone [60,78]. Industrial production is a major source: PTFE-associated nonpolymeric PFAS emissions in China were estimated at 1.06×10^5 kg in 2023, with 95.5% originating from the production stage [79]. Municipal WWTPs also remain persistent PFAS sources, and a U.S. meta-analysis reported a mean PFOA increase of 6.0 ± 1.6 ng L^{-1} from influent to effluent, with national mean effluent concentrations still at 8.4 ± 0.4 ng L^{-1} during 2013–2020 [80]. Additional evidence from e-waste recycling soils in Pakistan showed Σ41PFAS values of 7.43–367 ng g^{-1} dw, dominated by ultrashort-chain PFAS (56.8%), particularly trifluoroacetic acid [81].

The ongoing shift from legacy to replacement PFAS is also evident in biomonitoring and hotspot studies. In U.S. serum collected between 2003 and 2021, legacy PFAS declined markedly, whereas suspect screening revealed increasing replacement compounds such as F-53B, 6:2 DiPAP, and previously unreported chloroperfluorononylphosphonic acid [82]. In southern Lyon, a fluoropolymer/fluorotelomer industrial hotspot, 22 of 47 water samples exceeded 100 ng L^{-1} Σ77PFAS, maxima reached ~700 ng L^{-1}, and 67% of tap-water samples exceeded the EU 100 ng L^{-1} benchmark for Σ20PFAS; profiles were dominated by short-chain C4–C8 PFCAs, with the highest mean Σ77PFAS concentrations in groundwater (147 ng L^{-1}) [83]. Together, these findings confirm that PFAS occurrence is increasingly shaped by industrial source signatures, precursor transformation, and expanding replacement chemistry.

A comprehensive monitoring study in the Guadiaro River basin (southern Spain) illustrates how molecular EC occurrence can remain substantial even in moderately anthropized watersheds overlapping protected areas. Among 171 target organic contaminants analyzed in groundwater and surface waters, 25 were detected at least once, including pharmaceuticals, drugs of abuse, and PAHs. Cocaine and its main metabolite occurred in 85% and 95% of samples, respectively, at 0.001–0.18 and 0.004–0.6 μg L^{-1}, whereas pyrene was detected in all samples at 0.001–0.015 μg L^{-1} [84]. Notably, concentrations and calculated risk quotients were generally higher in groundwater, especially in detrital aquifers, indicating greater accumulation and slower hydrodynamics than in karst systems. This contrasts with the more episodic patterns often observed in surface waters and highlights groundwater as an important but less visible exposure compartment.

More broadly, replacement flame retardants, organophosphate additives, UV filters, pharmaceuticals, and steroid hormones are routinely detected in effluents and receiving waters, typically from ng L^{-1} to low μg L^{-1} levels, with UV filters occasionally reaching μg L^{-1} concentrations in heavily impacted recreational waters. Although many of these compounds occur at low dissolved concentrations, their biological relevance may still be substantial, particularly when parent compounds and transformation products co-occur [60].

A comparative European monitoring study further demonstrated the geographic variability and cumulative risk potential of multi-class endocrine-disrupting contaminants in urban rivers. Using a harmonized SPE–LC–MS/MS method, 26 EDCs were quantified in the R. Liffey, R. Thames, and R.

 doi:10.20944/preprints202604.0384.v1

Ter over a 10-week campaign. Maximum concentrations reached 4767 ng L^{-1} for tris(2-chloroethyl) phosphate (TCEP) in the Thames, while cumulative concentrations approached ~2000 ng L^{-1} in London compared with ~543 and ~436 ng L^{-1} in the Liffey and Ter, respectively. Caffeine, benzotriazole, and organophosphate flame retardants exhibited high detection frequencies, whereas steroid hormones generally remained in the low ng L^{-1} range. Relative risk quotient analysis identified caffeine and BPA as consistent high-risk contributors across sites, indicating that mixture-driven ecological risk depends not only on absolute concentration, but also on compound class and urban pressure [10].

This mixture perspective is reinforced at the global scale. A recent assessment across 60 countries compiled 4489 country-level mean concentrations covering 190 PPCPs, of which 184 were detected above MDL in at least one country Concentrations ranged from 0.01 ng L^{-1} for estriol to 94,307 ng L^{-1} for lamivudine, with a median concentration of 23.92 ng L^{-1} and cumulative national concentrations reaching 159.5 μg L^{-1} in Kenya. Ecological risk quotients identified hormones, NSAIDs, and antiepileptics as dominant contributors, accounting for more than 50% of total RQ in 54 countries, while ibuprofen, 17β-estradiol, carbamazepine, and estrone emerged as critical priority compounds [85]. Compared with the European river study, this global synthesis shows that mixture-driven prioritization is broadly consistent, although the magnitude of occurrence and risk remains strongly modulated by infrastructure, socioeconomic conditions, and hydrological dilution.

Coastal systems provide an additional perspective by integrating dissolved, particulate, and food-web processes. In the Bohai Sea, ΣPPCPs in seawater ranged from 57.5 to 309 ng L^{-1} across 25 stations, decreasing from coastal and estuarine zones toward the central basin, consistent with terrestrial and riverine inputs. Surface sediments contained 0.38–32.2 ng g^{-1} dw, while 53 PPCPs were detected in seawater and 40 in sediments. Antioxidants, bisphenols, and analgesic/anti-inflammatory drugs dominated seawater profiles, with benzotriazole reaching 109 ng L^{-1} [86]. In contrast to river monitoring focused mainly on dissolved concentrations, trophic magnification analysis in benthic food webs showed that ionization-corrected hydrophobicity (log Dow), rather than conventional log Kow, better predicted marine bioaccumulation.

High-throughput watershed monitoring highlights similar mixture complexity at the regional scale. In the Jingmi Water Diversion Canal (Beijing), a UPLC–MS/MS method targeting 323 PPCPs and pesticides detected 103 compounds, with antibiotics accounting for 25.2% of total detections. Mean total concentrations were significantly higher in winter (69.0 ng L^{-1}; range 0–1746.4 ng L^{-1}) than in summer (42.1 ng L^{-1}; range 0–389.3 ng L^{-1}), and urban sites consistently showed higher burdens than suburban sites [6]. Frequently detected compounds included caffeine, carbendazim, atrazine, diazepam, and desethyl atrazine, with detection frequencies up to 97.8%. Compared with the global assessment, this watershed-scale study shows that localized urban catchments can display similarly high mixture complexity, but with stronger seasonal amplification and sharper spatial contrasts [6,85].

Human biomonitoring and biota data further demonstrate that its occurrence in water can translate into internal exposure and bioaccumulation. In the SELF cohort, urinary concentrations of 16 phthalate metabolites, 7 phenols, 4 parabens, and triclocarban were quantified using online SPE coupled to isotope-dilution LC–MS/MS, with MDLs of 0.2–1.2 ng mL^{-1} for phthalates, 0.1–1.0 ng mL^{-1} for parabens, and 0.1–1.7 ng mL^{-1} for phenols. Principal component analysis identified mixture profiles dominated by phthalates, phenols, and parabens, with clear socioeconomic modulation of exposure patterns [87]. Likewise, in a national German fish survey downstream of WWTP discharges, only two pharmaceuticals were detected at low ng g^{-1} wet-weight levels, whereas synthetic musks reached much higher concentrations, up to 11,100 ng g^{-1} lipid weight for galaxolide [88]. Compared with dissolved-phase monitoring alone, these data show that lipophilic PCPs may exhibit much stronger bioaccumulation potential than many pharmaceuticals.

Finally, molecular EC occurrence is not restricted to surface waters, but extends to groundwater and to fluorinated chemical space that remains only partly captured by target methods. In the first large-scale assessment across 18 U.S. Principal Aquifers (>1000 sites), at least one compound was

 doi:10.20944/preprints202604.0384.v1

detected at 5.9% of public-supply sites and 11.3% of domestic-supply sites, with 34 distinct compounds identified overall, including bisphenol A, carbamazepine, sulfamethoxazole, meprobamate, and 1,7-dimethylxanthine. Although national detection frequencies were modest, vulnerability was higher in shallow wells and under conditions favoring rapid transport and limited attenuation [89]. At the same time, a multistrategy target and non-target HRMS investigation in the Liuyang River watershed identified 106 fluorinated compounds across surface waters and municipal effluents, including 36 confirmed PFAS and 23 compounds not previously reported in environmental matrices [24]. Compared with studies relying solely on predefined PFAS panels, this approach demonstrates that routine monitoring substantially underestimates fluorinated chemical diversity in urban river systems. Target PFAS concentrations ranged from 2.3–45.3 ng L^{-1} in winter surface waters and 6.1–65.6 ng L^{-1} in WWTP effluents, with short-chain PFCAs and PFSAs dominating [24]. Compared with conventional predefined PFAS panels, these findings confirm that routine monitoring substantially underestimates fluorinated chemical diversity in urban water systems.

2.2. Particulate Emerging Contaminants (Microplastics)

In aquatic systems, particulate emerging contaminants are dominated by MPs, including conventional polymer fragments and traffic-derived tire-wear particles. In contrast to molecular ECs, their environmental relevance depends not only on concentration, but also on particle size, polymer composition, surface properties, and their ability to act as both contaminants and vectors for sorbed chemicals and microorganisms.

Experimental evidence indicates that MPs can act as polymer-specific sorbents for cyanotoxins, with adsorption governed by intrinsic material properties rather than simple passive partitioning. Among the polymers tested, polystyrene (PS) consistently showed the highest sorption affinity, followed by PE and PVC, whereas PET exhibited minimal adsorption under comparable conditions. Sorption capacity was linked to polymer physicochemical properties, including glass transition temperature, amorphous-domain content, and surface morphology, while smaller particles (0.09–0.125 mm) showed enhanced adsorption because of their larger reactive surface area. Adsorption also varied between toxin congeners, reflecting differences in hydrophobicity and pH-dependent speciation. Together, these results show that MPs are not inert particles, but dynamic phases that can influence the partitioning and transport of molecular contaminants [35].

Beyond sorption processes, plastic debris can also function as biologically active microhabitats. Greenhouse polyethylene films supported a distinct plastisphere and harbored 295 ARGs, including high-risk genes, with evidence of ARG–MGE coupling. As opposed to cyanotoxin sorption, which is driven mainly by polymer properties, resistance enrichment on plastics appears to be governed by microbial colonization and selective antibiotic exposure. This comparison highlights the dual role of plastics as both physicochemical sorbents and biological vectors, extending their relevance beyond contaminant partitioning alone [36].

Urban stormwater runoff is a major land-based pathway for particulate ECs, mainly tire-wear particles (TWPs). In Queensland, Australia, stormwater MPs >25 μm ranged from 3.8 to 59 MPs L^{-1} in raw inlet water and from 1.8 to 32 MPs L^{-1} after treatment with a microlitter capture device, corresponding to 35–88% removal. TWPs accounted for about 95% of all particles, with concentrations of 2.5–58 TWPs L^{-1}, indicating clear traffic-related dominance in urban runoff. Compared with the polymer-specific interactions described above, this case emphasizes source strength and hydrological transport as the dominant controls on particulate occurrence in stormwater systems [90].

WWTPs, in turn, represent major sinks for MPs, but not necessarily final barriers. Most plants operating at secondary treatment or above remove more than 78% of influent MPs from the water phase into sludge. However, when biosolids are applied to land, this captured load is redistributed rather than eliminated; in Europe, land application has been estimated to return about 125–850 tonnes of MPs per million inhabitants per year. Across compiled datasets, median MP concentrations were

 doi:10.20944/preprints202604.0384.v1

225 MPs kg^{-1} dw in control soils, compared with 1106 MPs kg^{-1} dw in sludge-amended soils, while stabilized sludge itself reached a median of 18,923 MPs kg^{-1} dw [32]. Thus, compared with stormwater systems where capture devices can reduce particle loads before discharge, WWTP "removal" often represents transfer from water to solids, shifting the contamination burden from aquatic to terrestrial compartments.

Overall, these findings show that the environmental significance of MPs extends beyond their abundance alone and depends on polymer-specific interactions, biological colonization, and redistribution across water, sludge, soils, and stormwater pathways, all of which complicate their monitoring and interpretation.

3. Sampling and Sample Preparation Strategies

3.1. Sampling Considerations for Water Matrices

Sampling design is a major determinant of data quality for both molecular and particulate emerging contaminants, because occurrence patterns often depend on hydrology, source type, and temporal variability. Event-driven strategies are particularly important for contaminants showing short-lived storm peaks, whereas long-term and integrative designs are better suited to persistent or diffuse inputs.

For storm-responsive contaminants, temporally resolved sampling is essential. In urban receiving waters, grab and composite sampling during rain events coupled to UPLC–MS/MS have shown that 6-PPD-quinone (6-PPDQ) can rise rapidly during stormflow, reaching up to 2.3 μg L^{-1}, with peaks occurring a few hours after rainfall onset and remaining elevated above 2 μg L^{-1} for more than 10 h [16]. Additional storm-resolved monitoring in the Don River reported a 17–20 h lag between rainfall onset and maximum 6-PPDQ concentrations, with a peak of 2.30 μg L^{-1} followed by a near-plateau lasting 12–18 h [68]. Together, these studies show that single grab samples may miss both delayed maxima and exposure duration, making event-triggered and temporally resolved sampling indispensable for tire-derived contaminants.

A similar requirement applies to particulate ECs in stormwater. Event-triggered autosampling initiated at ≥2 mm rainfall per 30 min and flow >0.5 L s^{-1} enabled representative collection of 2.4–4 L per event for MP and TWP analysis under transient runoff conditions [90]. Composite storm sampling also allowed mass-load interpretation: paired monitoring of dissolved tire-wear chemicals by LC–MS/MS and particulate fractions by pyrolysis–GC–MS showed storm-related increases of >40× in summed additives, up to 2760 ng L^{-1} for 15 additives and 88 ng L^{-1} for 6-PPDQ, with event-scale loads approaching ~100 g $storm^{-1}$ for summed additives and ~3 g $storm^{-1}$ for 6-PPDQ [91]. Compared with single-timepoint sampling, such storm-resolved designs provide a more realistic characterization of both molecular and particulate exposure pulses.

Source-oriented solid sampling can further complement water monitoring when runoff alone does not capture the full congener space. In 20 end-of-life tires, seven target PPD-Q congeners summed to 9.30–95.0 μg g^{-1}, dominated by 6-PPD-Q, DTPD-Q, and DPPD-Q, while a fragment-guided non-target workflow identified an additional quinone, PTPD-Q, and several structural isomers. Notably, PTPD-Q was frequent in urban road dust (93% detection; median 5.07 ng g^{-1}), with concentrations comparable to DTPD-Q (5.56 ng g^{-1}), indicating that paired dissolved and particulate monitoring may still underestimate tire-derived risk drivers when emerging congeners are not included [92].

In contrast to storm-focused sampling, long-term routine monitoring is necessary for contaminants characterized by chronic or widespread baseline occurrence. Across 77 U.S. River sites sampled between 2013 and 2022 (12,547 samples), imidacloprid was detected in 44% of samples and at 72 of 77 sites, demonstrating that sustained multi-year programs are required to characterize persistent exposure rather than only episodic peaks [93]. Temporal variability in WWTP effluents similarly supports repeated sampling: in a biweekly campaign at a Virginia WWTP (n = 24), seasonal variation in several PFAS was observed, with PFPeA showing a statistically significant, although

 doi:10.20944/preprints202604.0384.v1

weak, correlation with temperature, suggesting that precursor biotransformation and operational variability can modulate effluent profiles over time [80]. Compared with event-driven strategies, these long-term designs are better suited to trend analysis and chronic exposure assessment.

Passive sampling provides a complementary time-integrative approach, particularly valuable for diffuse agricultural pollution and first-flush events. In an Eastern Mediterranean watershed, Chemcatcher passive samplers deployed before the first winter storm across 25 tributary and mainstream sites captured agrochemicals mobilized after about 6 months without rainfall. Combined LC–HRMS suspect screening and targeted LC–MS/MS identified 120 polar pesticides, of which 84 were quantified, with time-weighted average concentrations ranging from sub-ng L^{-1} to >1800 ng L^{-1} and cumulative site concentrations exceeding 2500 ng L^{-1}. Diuron, 2,4-D, imidacloprid, and tebuconazole were ubiquitous, and pesticide burdens correlated positively with agricultural land use. Compared with storm grab sampling, passive samplers enabled more robust watershed-scale comparison of tributary contributions and a better characterization of first-flush "toxic cocktails" [10].

The value of passive sampling is further illustrated in small agricultural streams. Using Chemcatcher samplers deployed over four 4-week periods in three agricultural headwater streams and one major river control, LC–HRMS analysis generated thousands of features in both ionization modes, while target analysis detected 44 of 99 monitored pesticides. In comparison with grab-based storm monitoring, passive sampling provided greater representativeness for chronic diffuse inputs and allowed clearer separation of spatial and seasonal effects, with site-specific variation dominating over seasonal trends [94]. These results show that passive sampling is especially useful for resolving low-level, non-point agricultural inputs where dilution variability and episodic pulses complicate conventional monitoring.

Overall, the choice of sampling strategy should reflect contaminant behavior and monitoring objectives. Event-triggered and composite sampling are most appropriate for hydrologically driven peaks, passive sampling is advantageous for diffuse and time-integrated exposure, and long-term repeated monitoring remains essential for identifying persistent contamination and temporal trends across water matrices.

3.2. Sample Preparation for Molecular Emerging Contaminants

Sample preparation for molecular ECs must be matched to both matrix complexity and analytical objective, since workflows optimized for trace-level quantification are not always appropriate for non-target discovery or particle-resolved characterization. In general, miniaturized extraction strategies are attractive for cleaner aqueous matrices, whereas solid, saline, lipid-rich, or highly complex samples require stronger enrichment, matrix disruption, or cleanup.

A representative miniaturized approach is the combination of solid–liquid extraction (SLE) and dispersive liquid–liquid microextraction (DLLME) coupled to LC–HRMS for lipophilic marine biotoxins. In seawater, direct DLLME of 12 mL using 450 µL chloroform and 500 µL methanol enabled effective preconcentration, with LODs as low as 0.0004 ng mL^{-1}. In contrast, mussel samples required prior SLE before DLLME, reflecting the need for matrix disruption and lipid-compatible extraction in biotic tissues. LOQs increased markedly to the ng g^{-1}–hundreds of ng g^{-1} range, highlighting matrix suppression and co-extraction effects [95]. Thus, compared with conventional SPE, DLLME offers low solvent consumption and rapid enrichment, but its selectivity may be limited in lipid-rich biological matrices.

For complex seafood matrices, matrix solid-phase dispersion (MSPD) offers a more integrated alternative by combining extraction and cleanup in a single step. In a Portuguese coast surveillance study of fish muscle, liver, and bivalves, MSPD coupled to LC-QTOF and GC-QTOF HRMS enabled broad multiclass screening, with pharmaceuticals mainly detected by LC-QTOF and industrial chemicals by GC-QTOF [96]. Compared with DLLME, MSPD is less miniaturized but more practical for heterogeneous biota extracts, especially when broad HRMS screening rather than targeted quantification is the priority.

 doi:10.20944/preprints202604.0384.v1

At the opposite end of the workflow spectrum, large-volume solid-phase extraction remains central for low-abundance unknowns in drinking water. In a non-target GC–HRMS investigation of alicyclic halocyclopentadienes, 5 L of source and finished drinking water were acidified to pH <1 and extracted on sequential XAD-2 and DAX-8 resins, followed by ethyl acetate elution and evaporation to 200 μL. Acidification improved recovery of neutral and weakly acidic halogenated species, while dual-resin extraction broadened capture of structurally diverse DBPs contributing to the unknown TOX fraction. Relative to miniaturized extraction, this approach is more labor- and solvent-intensive, but it is better suited to structural elucidation of previously unreported DBP classes [18].

For hydrophobic PCPs in sediment and biota, extraction is driven largely by strong lipid and solid-phase partitioning. Conventional LC–MS/MS remains the dominant approach for trace-level PCP analysis across water, sediment, and biota, although electrospray ionization is prone to signal suppression and enhancement in complex matrices, requiring matrix-matched calibration or isotope-dilution correction [52]. For sediment and fish tissues, Soxhlet and pressurized liquid extraction (PLE) are commonly applied, followed by cleanup steps such as gel permeation chromatography and silica or Florisil adsorption. This is especially important for UV filters, whose log Kow values of about 4–8 promote strong lipid co-extraction. Reported sediment methods illustrate the achievable sensitivity: triclosan has been quantified at 15.2 ng g^{-1} in marine sediments, while benzotriazole UV stabilizers have been reported at 0.18–24.0 ng g^{-1} with recoveries of 50.1–87.1%. Compared with simpler aqueous workflows, sediment and tissue preparation therefore requires more extensive cleanup to balance recovery and matrix removal [97].

Reported sediment concentrations further illustrate method sensitivity: triclosan was detected at 15.2 ng g^{-1} in marine sediments downstream of WWTP discharge following superheated liquid extraction, while microwave-assisted extraction of benzotriazole UV stabilizers yielded recoveries of 50.1–87.1% with environmental concentrations ranging from 0.18–24.0 ng g^{-1}. A separate PLE method using acetone:methanol (1:1) at 130 °C for 20 min reported triclosan levels of 4.4–35.7 ng g^{-1} in river sediments [97].

Targeted multi-matrix workflows for ubiquitous semi-volatile contaminants further illustrate that contamination control is often as important as extraction efficiency. In a validated LC–MS/MS method for eleven phthalate diesters, aqueous samples were acidified to pH 2, filtered, and extracted by polymeric SPE, whereas soil and municipal wastes were treated by repeated acetonitrile ultrasonication followed by SPE cleanup. Recoveries of 70–98% were achieved, outperforming Soxhlet extraction while reducing solvent consumption. However, the method also required isotopically labeled standards, baked glassware, phthalate-free consumables, and systematic procedural blanks to control laboratory background. Thus, in contrast to analyte-specific extraction challenges alone, ubiquitous contaminants demand preparation strategies that also minimize artefactual contamination [89].

The same principle applies when temporal representativeness is critical. During a COVID-19 peak monitoring campaign, 24 h composite influent and effluent wastewater samples were collected hourly, acidified to pH 2, stored at 4 °C in the dark, and processed within 2 weeks by SPE prior to LC–HRMS analysis. This example shows that sample preparation begins at preservation and storage, and that standardized pretreatment can be essential for comparability when wastewater loads vary rapidly over time [19].

For strongly sorbed contaminants in heterogeneous wastes, homogenization and extraction become especially important. In aged municipal landfill refuse (7–27 years), freeze-drying, homogenization, and solvent extraction enabled detection of 42 pharmaceuticals among 55 targets, with concentrations ranging from 0.30 to 116 μg kg^{-1}. Strong refuse–leachate partitioning for quinolones (Kd = 180–8100 L kg^{-1}; median 688 L kg^{-1}) further emphasized the need for rigorous preparation when contaminants are embedded in waste-derived matrices [98]. Compared with water samples, such solids require more aggressive homogenization and matrix disruption before chromatographic analysis is feasible.

 doi:10.20944/preprints202604.0384.v1

For engineered nanomaterials, sample preparation differs fundamentally from molecular extraction because the goal is to preserve particle number, size, and transformation state rather than transfer analytes into solvent. In landfill leachates, nanoparticle tracking analysis enabled simultaneous assessment of particle-size distribution, number concentration, and derived mass distribution for 100 nm Au ENMs, with matrix-dependent calibration required for accurate quantification in synthetic and natural leachates [99]. Advanced particle-resolved workflows such as single-particle ICP–MS coupled with asymmetric flow field-flow fractionation further showed that transformation studies, such as AgNP sulfidation, require preservation of the entire particle mass distribution and minimization of artefactual aggregation or dissolution [100]. More broadly, ultrafiltration, ultracentrifugation, cloud-point extraction, and pyrophosphate-based extraction have been reviewed as key pretreatment strategies, with enrichment factors up to 10^2 and ng L^{-1} detection limits when coupled to ICP–MS [11]. Compared with bulk metal analysis, these particle-resolved approaches are essential for distinguishing engineered nanoparticles from natural colloids and for tracking aggregation and transformation.

PFAS sample preparation is highly matrix- and objective-dependent. For regulatory analysis, polymeric SPE coupled with LC–MS/MS remains the standard approach, especially for aqueous samples, because it provides robust enrichment and good compatibility with standardized workflows. However, target analysis alone may underestimate the total fluorinated burden in complex matrices. In treated wastewater, recoveries ranged from 61 to 105%, whereas target analysis explained only 1.5% of total organic halogen. Thus, PFAS sample preparation should be selected according to both matrix type and analytical purpose [78]. However, ultrashort-chain PFAS such as trifluoroacetic acid have been reported at up to 12.4 μg L^{-1} and may account for as much as 98% of total PFAS mass in some drinking waters, illustrating a major analytical blind spot when workflows focus mainly on longer-chain compounds [101]. In industrially impacted waters, polymeric SPE can also serve as a front-end to HRMS: in a fluoropolymer-affected region south of Lyon, 47 water samples were processed by SPE with surrogate standards prior to UHPLC–Orbitrap HRMS analysis of 77 target PFAS plus suspect screening [83]. By contrast, solid consumer-product matrices such as reusable hygiene textiles required solvent-based extraction combined with dual-platform LC–MS/MS and GC–MS workflows to cover both ionic and neutral PFAS while controlling fluorine background contamination [102]. For saline waters, reversed-phase polymeric SPE combined with standard addition provided robust quantification of highly polar sweeteners, with recoveries of 73.5–128.4% and RSDs <9.2%, demonstrating how salinity-specific matrix effects can require different calibration strategies even when the sorbent format remains similar [53].

Bulk fluorine metrics provide a complementary perspective to compound-resolved workflows. EPA Method 1621 determines adsorbable organic fluorine through adsorption onto granular activated carbon, combustion at ≥1000 °C, and fluoride quantification by ion chromatography, with recoveries of 45–147% and an MDL of 1.5 μg F L^{-1} [60]. Although it lacks molecular specificity, Adsorbable Organic Fluorine (AOF) helps contextualize the substantial fraction of fluorinated organic matter not explained by target PFAS analysis.

Overall, these examples show that sample preparation must be tailored not only to contaminant class and matrix complexity, but also to the analytical purpose itself. Miniaturized extraction is advantageous for clean aqueous matrices, large-volume enrichment is more appropriate for low-abundance unknowns, extensive cleanup is essential for solids and biota, and particle-resolved pretreatment is indispensable for nanomaterials. Thus, extraction scale, sorbent chemistry, cleanup intensity, and analytical resolution must all be aligned with whether the goal is compliance monitoring, quantitative multi-residue analysis, or structural elucidation of previously unrecognized ECs.

 doi:10.20944/preprints202604.0384.v1

3.3. Sample Preparation for Particulate Emerging Contaminants (Microplastics)

Sample preparation for MPs and NPs must combine size-resolved isolation with effective removal of organic interferences while minimizing procedural contamination. Unlike dissolved molecular ECs, particulate workflows require a careful balance between sufficient matrix digestion and preservation of polymer integrity. As a result, most protocols follow a stepwise scheme involving particle capture, matrix cleanup, and density-based enrichment before spectroscopic or thermal identification. A schematic overview of these strategies is shown in Figure 1.

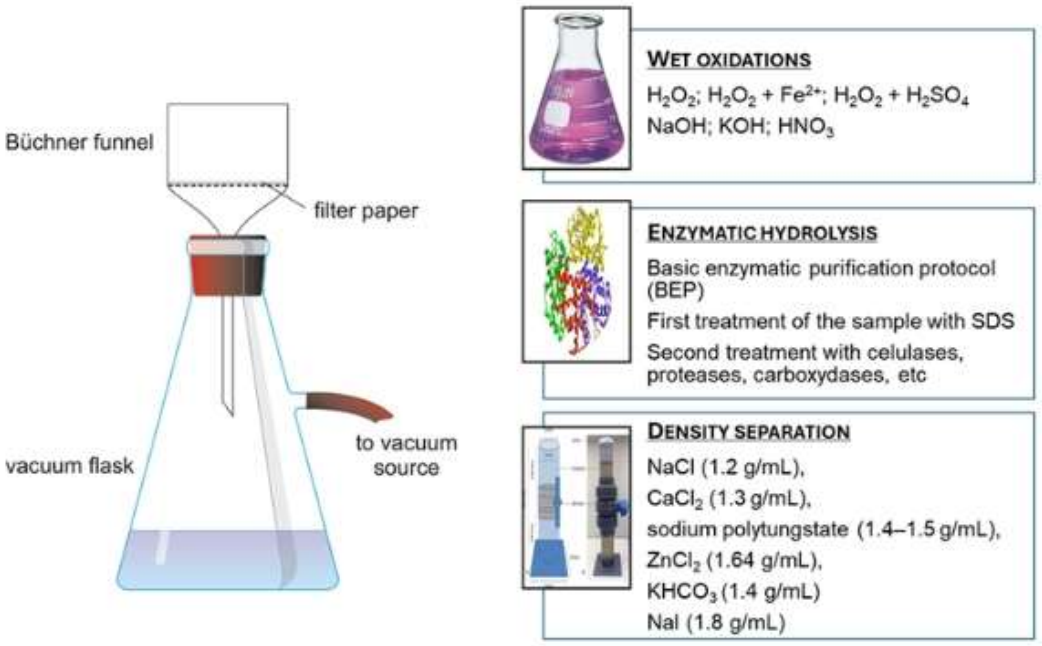

Figure 1. Representative extraction and clean-up workflow for MPs in complex environmental matrices. Common pretreatment strategies include wet oxidation for the removal of organic matter, enzymatic digestion for selective degradation of biological matrix components, and density separation for the enrichment of plastic particles prior to spectroscopic or thermal identification.

In wastewater matrices, one approach combined microfiltration/ultrafiltration with H_2O_2 digestion and sequential filtration on 1000, 50, and 1 μm stainless-steel membranes prior to pyrolysis–GC–MS analysis. This workflow enabled retention of both MP and NP fractions after oxidative cleanup, with total MP and NP mass concentrations decreasing from 26.2 and 11.3 μg L^{-1} in influent to 1.8 and 0.7 μg L^{-1} in effluent, corresponding to 93% and 94% removal, respectively [103]. Compared with particle-counting strategies, this example highlights the importance of high-throughput filtration combined with digestion when polymer mass is the target metric.

For low-turbidity drinking or tap water, simpler front-end preparation may be sufficient. Direct size-selective capture using 25 μm stainless-steel filters mounted on taps, followed by micro-IR confirmation, reduced handling losses and background contamination and provided a defensible strategy when the target size window was clearly defined [104]. Thus, compared with wastewater, cleaner matrices may require less aggressive pretreatment and benefit from direct filtration approaches.

Solid environmental matrices such as soil, sediment, and sludge generally require more intensive dismantling to release embedded polymers before analysis. A protocol based on tetramethylammonium hydroxide digestion, ethanol washing to remove natural organic matter, and dichloromethane dissolution with ultrasonication achieved recoveries of 80–91% across PS, PE, PP, PMMA, PVC, and PET, with pyrolysis–GC–MS detection limits of 2.3–29.2 μg g^{-1} [60]. These results

 doi:10.20944/preprints202604.0384.v1

emphasize that extraction efficiency is strongly matrix- and polymer-dependent, making recovery validation essential for heterogeneous solids.

Tire road wear particles (TRWPs) require additional adaptation because their density (1.3–1.7 g cm^{-3}) often exceeds the limits of conventional NaCl separation. A two-stage density separation using saturated NaCl ($\varrho \approx 1.2$ g cm^{-3}) followed by sodium polytungstate ($\varrho = 1.9$ g cm^{-3}) recovered up to 98% of TRWPs below 1.9 g cm^{-3}. Alkaline digestion with NaOH or KOH preserved microrubber structure, whereas H_2O_2 and NaOCl caused deformation. Because carbon black interferes with vibrational spectroscopy, confirmation required SEM and pyrolysis–GC–MS, with isolated TRWPs ranging from 63 to 500 µm [105]. Compared with conventional MP workflows, tire-derived particles therefore demand denser separation media and greater reliance on thermal or electron-based confirmation.

A similar issue arises in stormwater, where particle-rich matrices and dense fragments complicate recovery. A validated workflow combined filtration on 25 µm stainless-steel filters, oxidative digestion with 30% H_2O_2, high-density separation using NaI (1.8 g cm^{-3}), and Rose-Bengal staining prior to stereomicroscopic screening of suspected MPs >25 µm [90]. Compared with low-density separations alone, this approach is better suited for recovering TWPs and other dense anthropogenic particles that would otherwise be underestimated.

At the same time, newer analytical approaches aim to reduce the wet-chemistry burden while extending detection to smaller particles. IR photothermal heterodyne imaging has achieved a spatial resolution of about 300 nm with minimal sample preparation, and Raman spectroscopy combined with machine-learning classification reported 99% identification accuracy for NPs and >97% accuracy in spiked tap-water validation [60]. Compared with conventional digestion and density-separation workflows, these approaches shift selectivity toward instrumental resolution and chemometric classification, potentially reducing losses, contamination risks, and recovery bias associated with extensive pretreatment.

Overall, sample preparation for particulate ECs is more strongly constrained by particle properties than is the case for dissolved analytes. Wastewater and solid matrices generally require digestion and enrichment, drinking water can often be addressed by direct filtration, and tire-derived particles demand denser separation and alternative confirmation methods. This matrix- and particle-specific preparation remains essential for reliable MP and NP occurrence data.

4. Analytical Strategies for Molecular Emerging Contaminants

The analytical determination of molecular ECs in aquatic environments requires methods that combine sensitivity, selectivity, and structural information across chemically diverse compounds occurring at trace levels. Over the last decade, analytical strategies have expanded from strictly targeted quantification toward multidimensional high-resolution and non-target workflows. Nevertheless, targeted LC–MS/MS remains the core quantitative approach for predefined analyte lists and regulatory monitoring.

4.1. Targeted LC-MS/MS Approaches

Targeted LC–MS/MS, typically based on triple-quadrupole instruments operating in multiple reaction monitoring mode, remains the reference technique for quantitative determination of priority ECs. Its main strengths are high sensitivity, excellent selectivity, and compatibility with interlaboratory standardization, generally allowing quantification from ng L^{-1} to sub-ng L^{-1} levels for predefined analytes.

Recent developments have expanded targeted LC–MS/MS toward chemically challenging classes such as PFAS. A multidimensional configuration integrating large-volume direct injection with dynamic heart-cutting between reversed-phase and HILIC–ion-exchange columns enabled simultaneous quantification of 60 PFAS without offline SPE, thereby improving coverage from ultrashort- to long-chain homologues. Matrix-specific LOQs were ≤1 ng L^{-1} for most analytes in

 doi:10.20944/preprints202604.0384.v1

surface and seawater, although trifluoroacetic acid showed a much higher LOQ (~500 ng L^{-1}) because of background contamination [22]. Compared with conventional SPE–RP–LC–MS/MS workflows, this setup reduces extraction bias and broadens polarity coverage, while still remaining limited to predefined target compounds.

Regulatory standardization has further strengthened the role of targeted LC–MS/MS. EPA Method 1633 enables determination of 40 PFAS in aqueous, solid, biosolid, sediment, and tissue matrices using SPE–LC–MS/MS with isotopically labeled standards, achieving recoveries of 45–145% and LOQs of 1–100 ng L^{-1}, most commonly 1–4 ng L^{-1} in water [60]. Similarly, Draft EPA Method 1634 for 6-PPDQ in water reports recoveries of 78–96% and an MDL of 0.43 ng L^{-1}, whereas Draft EPA Method 1628 for PCB congeners uses low-resolution GC–MS with SIM and reports MDLs of 0.2–5.0 ng L^{-1} in water [60]. These developments show that targeted methods continue to expand toward newly recognized EC classes while maintaining strong regulatory comparability.

Beyond regulatory methods, targeted LC–MS/MS is increasingly adapted to difficult analytes and contamination-prone workflows. Phthalate diesters illustrate this well: a validated multi-matrix LC–MS/MS method quantified eleven phthalates in surface water, landfill leachate, soils, and municipal wastes with detection limits down to 0.2 ng L^{-1} and precision below 5% RSD [106]. Importantly, the workflow incorporated a chromatographic delay column to displace instrument-derived phthalate contamination, together with blank correction, isotopically labeled standards, and phthalate-free consumables. This example highlights that, for ubiquitous contaminants, analytical robustness depends as much on contamination control as on instrumental sensitivity.

Targeted LC–MS/MS also remains indispensable for multi-compartment exposure studies. In lysimeter-grown tomatoes irrigated with treated wastewater, validated UHPLC–QqLIT-MS/MS workflows combined with Oasis Prime HLB extraction were used to monitor 27 contaminants across irrigation water, soil, roots, leaves, stems, and fruits [38]. Under non-spiked irrigation, only carbamazepine was detected in fruits above LOQ (22 ng g^{-1}), whereas up to 17 compounds accumulated in roots at ng g^{-1} levels; spiking experiments at 1 mg L^{-1} further confirmed compound-specific translocation to edible tissues. Similarly, a 21-day semi-static assay with Corbicula fluminea exposed to 6-PPD or 6-PPDQ used triple-quadrupole LC–MS/MS to verify water concentrations with an MDL of 0.01 μg L^{-1} for both analytes [107]. Such applications underline the continuing value of triple-quadrupole platforms for quantitatively linking external exposure to tissue-specific accumulation.

At the same time, targeted LC–MS/MS can now be scaled toward broader exposome-level panels. A next-generation human biomonitoring workflow using 96-well SPE and LC–MS/MS quantified more than 230 biomarkers across urine, plasma, and serum, with extraction recoveries and matrix effects largely within 60–130% and intraday/interday RSDs below 30%. LODs below 0.1 ng mL^{-1} were achieved for 59–80% of analytes, supporting high-throughput large-cohort studies [108]. Compared with classical priority-pollutant methods, such workflows expand analytical breadth substantially, although they remain confined to known and predefined targets.

This limitation becomes particularly evident for structurally diverse toxin families. In cyanotoxin analysis, more than 250 microcystin congeners have been described, yet routine targeted monitoring generally focuses on a small subset, often dominated by MC-LR [57]. The high-resolution analysis of algal dietary supplements revealed 35 additional minor congeners beyond those routinely targeted by LC–MS/MS, while bioassay-based methods such as ELISA and protein phosphatase inhibition assays often yielded higher equivalent concentrations because they captured cumulative biological activity rather than a restricted target list [109]. Thus, although targeted LC–MS/MS provides excellent sensitivity and structural specificity, it can systematically underestimate total toxin burden when congener diversity is high.

The same tension between quantitative robustness and restricted coverage is seen across other EC classes. Targeted UPLC–ESI(+)-QQQ-MS has been used for long-term monitoring of 21 quaternary ammonium compounds in influent, effluent, and biosolids, achieving low ng L^{-1} detection limits in water and low μg kg^{-1} in solids while prioritizing homolog-specific surveillance over the

 doi:10.20944/preprints202604.0384.v1

expansion of chemical space [110]. Small, highly polar food-additive ECs such as artificial sweeteners have also been quantified by SPE–UPLC–ESI(−)–QQQ with LODs of 0.006 mg L^{-1} and LOQs of 0.01 mg L^{-1} [53]. At the other end of the scale, nationwide U.S. river monitoring of imidacloprid across 12,547 samples from 77 sites used direct aqueous injection LC–MS/MS and showed detections in 44% of samples, with 39% exceeding the EPA chronic aquatic invertebrate benchmark of 10 ng L^{-1} [93]. Together, these examples show that triple-quadrupole methods remain highly versatile across EC classes, matrices, and monitoring scales.

Complementary rapid-screening tools can reduce analytical workload when full LC–MS/MS confirmation is not required. Multiplex competitive lateral flow immunoassays have enabled simultaneous detection of okadaic acid, saxitoxin, and domoic acid in shellfish with LODs of 0.1, 1.1, and 4.4 ng mL^{-1}, respectively, and recoveries of 85.8–131.4% in spiked mussel extracts [111]. Electrochemical biosensors for cyanotoxins, particularly microcystin-LR, have reported exceptionally low detection limits in optimized nanocomposite designs and response times as short as 5–20 min in some saxitoxin platforms [112]. However, unlike LC–MS/MS, these methods generally provide limited structural confirmation and are therefore better viewed as rapid, semi-quantitative complements rather than replacements.

Overall, targeted LC–MS/MS remains the quantitative backbone of molecular EC analysis thanks to its sensitivity, selectivity, and regulatory compatibility. Its main limitation, however, is intrinsic restriction to predefined analyte panels. As contaminant space continues to expand through transformation products, replacement PFAS, low-abundance congeners, and uncharacterized toxins, targeted LC–MS/MS remains indispensable for robust quantification but increasingly requires support from HRMS, suspect screening, and effect-based tools to capture the full diversity of molecular ECs.

4.2. High-Resolution Mass Spectrometry (HRMS)

High-resolution mass spectrometry (HRMS), most commonly implemented as LC–HRMS on Orbitrap or QTOF platforms, has greatly expanded environmental water analysis by enabling accurate-mass measurement, full-scan acquisition, and broad chemical profiling. As opposed to targeted LC–MS/MS, HRMS supports both suspect screening and non-target screening, allowing simultaneous interrogation of known, expected, and previously unreported contaminants within a single run.

One of the key strengths of HRMS is its ability to combine quantitative determination with structural expansion. For example, DLLME coupled to LC–QTOF–HRMS enabled simultaneous targeted quantification and suspect screening of eight regulated lipophilic marine biotoxins in seawater and mussel samples. Accurate-mass measurements within ±5 ppm, auto-MS/MS acquisition, and a suspect database containing 93 derivatives supported multidimensional annotation based on precursor mass, fragment ions, and mass-accuracy thresholds. Detection limits ranged from 0.0004–1.7 ng mL^{-1} in seawater and 0.06–119 ng g^{-1} in mussels, illustrating how HRMS can combine regulatory quantification with structural exploration of toxin derivatives in complex marine matrices [95]. A similar expansion of chemical space was demonstrated in Portuguese coastal biota, where MSPD extracts analyzed by LC-QTOF and GC-QTOF HRMS enabled tentative identification of 176 compounds and confirmation of 77 with standards, while also separating profiles according to tissue, sampling area, and campaign [96]. Compared with targeted workflows, these examples show the broader structural reach of HRMS in complex food-web relevant matrices.

HRMS is also particularly valuable for elucidating treatment-induced transformation products that lie outside predefined target lists. In acesulfame degradation experiments, UHPLC–QqQ–MS was used for kinetic monitoring, whereas UHPLC–QTOF–HRMS identified chlorinated transformation products formed specifically under UV/monochloramine treatment. Under UV irradiation, 92% degradation was achieved, while monochloramine increased the apparent degradation rate and generated oxidant-specific products absent in UV-only systems [113]. Similarly,

 doi:10.20944/preprints202604.0384.v1

LC–HRMS suspect workflows coupled with transformation-product prediction and retention-time prediction enabled the identification of 114 pharmaceuticals and transformation products in WWTP samples during a COVID-19 peak, including 13 TPs not previously reported in wastewater [19]. HRMS has also proved valuable for tracking reactive intermediates and extending contaminant discovery to non-aqueous matrices. For example, UHPLC–QTOF–MS was used to follow chlorinated intermediates formed from bisphenol analogues during disinfection, while complementary UHPLC–QqQ–MS quantified BDA formation, showing that BDAs formed preferentially under neutral conditions and were inhibited by chloramination, thereby illustrating disinfectant-dependent DBP formation pathways [114]. In parallel, LC–MS-based screening of aged municipal landfill refuse enabled quantification of 55 pharmaceuticals, of which 42 were detected at 0.30–116 μg kg^{-1}, demonstrating that HRMS-compatible workflows can also extend contaminant profiling to complex solid waste reservoirs [98]. Together, these examples highlight a major contrast with triple-quadrupole methods: HRMS not only tracks parent removal, but also captures chemical space expansion during treatment and in secondary source matrices.

A further advantage of HRMS is its usefulness in mechanistic and source-diagnostic analysis. Compound-specific isotope analysis, typically performed by GC-IRMS or LC-IRMS, provides process-level evidence distinguishing dilution or sorption from true transformation by interpreting isotope fractionation of elements such as C, H, N, and Cl. Although not a conventional full-scan HRMS workflow, CSIA complements HRMS by clarifying reaction pathways in groundwater contamination, diffuse pesticide pollution, and water-treatment systems [115]. More generally, this illustrates that advanced mass-spectrometric strategies increasingly move beyond concentration data alone toward process interpretation.

A major recent development has been the integration of ion mobility spectrometry (IMS) with HRMS. By providing collision cross section (CCS) values as an orthogonal structural descriptor alongside m/z, retention time, and MS/MS fragmentation, LC–IMS–HRMS improves the discrimination of structurally similar compounds, especially isomers. This is particularly relevant for PFAS, where high structural similarity often complicates confident annotation. Updated guidance now incorporates CCS evidence into standardized confidence levels for LC- or GC-IMS-HRMS identifications, thereby improving harmonization and transparency in PFAS reporting [116]. In environmental applications, UPLC–cIMS–QTOF–HRMS enabled annotation of 678 chemicals in estuarine sediments, including human and veterinary drugs (8.7%), food additives (6.5%), pesticides (2.8%), and PFAS (1.9%), while hotspot patterns reflected diffuse inputs and deposition zones [117]. Likewise, LC–IMS–QTOF analysis of 156 U.S. serum samples collected between 2003 and 2021 combined accurate mass, retention time, and CCS matching to support the quantification of 19 PFAS and suspect screening of replacement compounds such as F-53B, 6:2 DiPAP, and chloroperfluorononylphosphonic acid [82]. Compared with LC–HRMS alone, the IMS dimension therefore improves structural discrimination and retrospective interpretation.

HRMS has been especially transformative for PFAS analysis because it reveals how much fluorinated chemical space remains unresolved by target methods. Recent investigations identified 35 novel PFAS classes in commercial fluorinated products using UPLC–Orbitrap HRMS/MS, while newly discovered PFECAs accounted for 27–95% of total PFAS in industrial effluents, with individual compounds reaching 447 μg L^{-1} in effluent and 670 ng L^{-1} in nearby surface waters [118]. In drinking water, ultrashort-chain PFAS such as trifluoroacetic acid reached 12.4 μg L^{-1} and contributed up to 98% of total PFAS burden in some samples [119]. HRMS has also expanded PFAS profiling in complex solids: in e-waste recycling soils, LC–Orbitrap HRMS detected nine CF_3-containing emerging PFAS beyond target panels, while TOP assay validation linked several of them directly to trifluoroacetic acid (TFA) formation [81]. Compared with predefined target workflows, these HRMS-based approaches reveal substantial precursor contributions and under-monitored short-chain species that strongly affect fluorine mass balance.

Complementary multidimensional resources further strengthen HRMS interpretation. An open collision cross-section (CCS) library containing 556 organic micropollutants measured in both

 doi:10.20944/preprints202604.0384.v1

ionization modes improved discrimination of isobaric and isomeric compounds and supported PFAS profiling in complex mixtures such as aqueous film-forming foams [120,121]. In parallel, ^19F-NMR has emerged as a complementary technique for quantifying total fluorinated burden independently of chromatographic retention or ionization efficiency. Although its detection limits remain much higher than those of LC–MS methods and its structural resolution is limited in mixtures, ^19F-NMR provides a matrix-independent measure of total PFAS that can contextualize LC–HRMS findings [122].

Finally, HRMS datasets gain additional power when combined with chemometric decomposition. In a passive-sampling campaign across three small streams and one river, full-scan Orbitrap analysis followed by variance-based reduction and ASCA modeling separated spatial and temporal components of variation, while PLS-DA and volcano-based prioritization identified 223 site-specific and 45 season-specific discriminating features. Notably, the non-target dataset provided clearer separation of pollution fingerprints than target-only analysis, illustrating how HRMS transforms feature-rich data into ecologically interpretable contamination patterns [94].

Overall, HRMS extends analytical coverage far beyond predefined target panels by coupling accurate mass, full-scan acquisition, structural annotation, and retrospective analysis. Its main strengths lie in suspect and non-target screening, transformation-product discovery, PFAS structural expansion, and multidimensional workflows integrating IMS, chemometrics, or complementary total-fluorine approaches. Compared with targeted LC–MS/MS, HRMS offers substantially broader chemical-space coverage, although annotation confidence, data complexity, and the need for advanced processing remain important limitations.

4.3. Non-Target and Suspect Screening Approaches

Suspect screening (SS) and non-target screening (NTS) extend analytical coverage beyond predefined compound lists by exploiting full-scan LC–HRMS or LC–IMS–HRMS datasets. In contrast to targeted LC–MS/MS, these approaches rely on integrated interpretation of accurate mass, isotopic pattern, MS/MS fragmentation, retention behavior, and, where available, collision cross section (CCS) values. Their main advantage is the ability to detect both expected and previously unreported contaminants within the same dataset, although annotation confidence depends strongly on the quality of reference databases, spectral libraries, and filtering criteria.

PFAS analysis provides one of the clearest demonstrations of the value of suspect and non-target workflows. In a European hotspot setting, combined target screening of 77 PFAS and suspect screening of about 120 additional PFAS using UHPLC–HRMS (Q Exactive Orbitrap) expanded fluorinated chemical space well beyond standard drinking-water monitoring panels. Candidate suspects were extracted within ±10 ppm and filtered by blank subtraction and intensity thresholds, while retention-time homolog patterns, isomeric peak shapes, and HRMS/MS comparison with previously characterized AFFF formulations strengthened identification confidence [83]. This strategy revealed industrially consistent precursor and fluorotelomer signatures, including N-SPAmP-FHxSAA, bistriflimide, and fluorotelomer betaines/sulfonates, which would be missed by conventional Σ20 PFAS target lists [83].

Because PFAS structural diversity now spans thousands, and potentially far more, candidates, harmonized confidence frameworks have become essential. Updated PFAS-specific guidance proposes a five-level confidence system integrating accurate mass, MS/MS evidence, retention time, and CCS values, while emphasizing that tolerances for these parameters should remain instrument- and method-specific rather than universally fixed [116]. In practice, CCS reproducibility is generally good within a single IMS platform, but differences between technologies such as drift-tube and traveling-wave IMS require transparent reporting of platform-specific tolerances. Thus, compared with conventional suspect screening based only on mass and fragments, multidimensional frameworks can improve annotation consistency but remain limited by the availability of reliable CCS libraries.

 doi:10.20944/preprints202604.0384.v1

To strengthen this multidimensional evidence layer, dedicated tools such as FluoroMatch IM have been developed. This vendor-neutral platform integrates CCS matching, molecular formula prediction, homologous series detection, mass-defect filtering, and accurate-mass database matching, thereby reducing false discovery rates in LC–IMS–HRMS datasets [123]. A broader example of fluorinated-compound screening was reported for an urban river system using integrated target and non-target LC–HRMS workflows. By combining target analysis of 45 PFAS with library matching against more than 7,096 fluorinated compounds, homologous-series analysis (CF_2, CF_2O, CF_2CH_2, C_3F_6O series), molecular networking, analogue searching, and reaction-database-guided annotation, the workflow identified 106 fluorinated compounds across surface waters and municipal effluents, including 36 confirmed PFAS and 23 compounds not previously reported in environmental matrices [24]. Compared with CCS-focused PFAS workflows, this strategy relied more heavily on hierarchical evidence layering and spectral propagation to expand fluorinated chemical space while controlling false positives.

In contrast to these broad fluorinated workflows, marine toxin analysis illustrates a more constrained but highly structured form of suspect screening. A curated library of 93 toxin derivatives was integrated into a targeted feature-extraction workflow using predefined ±5 ppm mass tolerances and a minimum match score threshold of 80% [95]. This ensured transparent and reproducible filtering of candidate features, but the workflow remained inherently dependent on prior database inclusion. Compared with algorithm-assisted networking or IMS-enhanced PFAS workflows, such strategies emphasize controlled suspect expansion rather than open-ended discovery [95].

At the multiclass level, complementary LC–HRMS and GC–HRMS platforms have demonstrated the value of broad suspect screening for mixture characterization across environmental, food, and human matrices. In one large-scale study, pooled wastewater, fish, and human serum samples were analyzed using both UHPLC–Orbitrap and GC–HRMS, and spectral matching against MoNA and MassBank enabled annotation of 547 compounds at Schymanski confidence levels 1–3, including 63 confirmed at Level 1. Wastewater showed the highest chemical diversity (341 compounds), whereas fish samples contained 25–27 detected compounds. The combined use of LC and GC platforms expanded chemical space coverage substantially, achieving about 99% detectability of QA/QC compounds when both techniques were applied together [124]. Compared with PFAS-specific IMS-supported workflows, this approach prioritizes broad mixture coverage rather than fine structural discrimination of closely related isomers.

A complementary hybrid strategy combines total fluorine screening with compound-specific confirmation. In reusable feminine hygiene products, particle-induced gamma emission identified intentional fluorination in 33% of period underwear and 25% of reusable pads, after which LC–MS/MS and GC–MS confirmed PFAS in all extracted samples, with 6:2 and 8:2 fluorotelomer alcohols dominating. Products classified as non-intentionally fluorinated contained Σ42PFAS of 21–880 ng g^{-1}, whereas intentionally fluorinated products contained 48–2205 ng g^{-1} [102]. This workflow illustrates how broad elemental-level screening can prioritize suspect materials, while compound-resolved mass spectrometry provides molecular confirmation and semi-quantitative assessment.

Another large-scale application of combined target and LC–HRMS non-target analysis was demonstrated in longitudinal monitoring of two major German river systems. In contrast to class-specific PFAS workflows or broad multiclass LC–GC suspect screening, this study combined quantitative LC–MS/MS with Orbitrap-based LC–HRMS and feature-based molecular networking to examine mixture evolution along urban gradients. Rather than emphasizing annotation counts alone, the workflow linked chemical features to catchment characteristics such as wastewater input and land cover, while molecular networking propagated structural information to spectrally related but previously unannotated features [125]. This example shows that large-scale NTS can support both compound discovery and source attribution, and longitudinal mixture interpretation.

Similar SS/NTS logic has been applied to less studied contaminant classes in remote systems. In Arctic soils and sediments, target and suspect screening of polyhalogenated carbazoles (PHCZs) revealed Σ11PHCZ concentrations of 0.06–165.6 ng g^{-1} dw in soils and 1.2–4.5 ng g^{-1} dw in sediments,

 doi:10.20944/preprints202604.0384.v1

with 100% detection frequency [126]. These findings confirm that dioxin-like emerging contaminants can occur even in remote environments and illustrate how SS/NTS approaches expand analytical scope beyond conventional POP monitoring frameworks.

The same expansion is increasingly important for solid environmental matrices. In sewage sludge, nanoLC–Orbitrap HRMS combined with semi-quantitative modeling enabled broad contaminant profiling in biosolids, linking Schymanski-based structural confirmation with isotopically assisted response-factor estimation [127,128]. Compared with water-based multiclass screening, these workflows place greater emphasis on sensitivity and matrix-adapted extraction, but still face uncertainty arising from semi-quantification and chromatographic bias toward moderately hydrophobic compounds [128].

Non-target workflows have also become more selective through reactivity-driven prioritization. A recent approach combining stable-isotope labeling with glutathione probes and HPLC–HRMS screened chlorinated and chloraminated waters for electrophilic DBPs, reducing >50,000 raw features to 255 isotopically paired adducts and ultimately identifying 202 DBPs, including 193 newly reported compounds. Mechanistic grouping further distinguished chlorinated substitution products from unsaturated addition products. Compared with broad multiclass suspect screening, this strategy narrows chemical space toward biologically reactive contaminants, increasing toxicological relevance, although it remains limited to probe-reactive species and is not inherently quantitative [129].

GC–HRMS has likewise expanded non-target analysis for volatile and halogen-rich DBPs. In chlorinated and chloraminated waters, high-resolution EI-TOF-MS combined with 5 L XAD-resin enrichment enabled identification of alicyclic HCPDs through accurate mass and characteristic Cl/Br isotope patterns, with six compounds detected exclusively after disinfection. Complementary GC×GC improved isomer separation, although Level 1 confirmation still required authentic standards. Compared with LC–HRMS suspect workflows, this GC–HRMS configuration is better suited to volatile DBPs contributing to the unresolved TOX fraction [18].

The scale of this unresolved DBP chemical space is illustrated by recent curation efforts. A comprehensive database compiling 6310 DBPs reported between 1974 and 2022 classified only 651 as confirmed, whereas 1478 were identified and 4142 remained proposed structures. This imbalance highlights a central limitation of SS/NTS workflows: full-scan acquisition greatly expands candidate discovery, but exposure-relevant interpretation remains constrained by standard availability, confidence harmonization, and transferability from laboratory formation studies to real environmental samples [4].

Effect-directed analysis (EDA) coupled with HRMS has been especially powerful for toxicant discovery. The identification of 6-PPDQ as the driver of coho salmon mortality is a well-known example, linking HRMS-based structural elucidation to an acute LC_{50} of 95 ng L^{-1} and subsequent urban stormwater concentrations up to 2.3 μg L^{-1} [60]. Wide-scope HRMS screening of snowmelt similarly detected 489 chemicals, including tire-derived transformation products from 1.3 ng L^{-1} to 75 μg L^{-1}, highlighting transient pulses that targeted analysis might overlook [130]. More recently, a fragmentation-pattern-based HRMS workflow using diagnostic ions and neutral-loss criteria enabled recognition of six known and three previously unreported PPD-quinones across tire tissue, $PM_{2.5}$, and surface soils, including first quantification of 8PPD-Q and 66PD-Q. Compared with earlier suspect-screening strategies, this diagnostic-fragment approach improves structural confidence for rubber-derived transformation products lacking commercial standards [25]. A related development is the integration of bioassay guidance into suspect and non-target workflows. In drinking water, virtual effect-directed analysis (vEDA) coupled LC–HRMS and GC–HRMS datasets with ERα-CALUX bioassays to prioritize features associated with observed biological activity rather than structural plausibility alone [131]. Similarly, in cyanotoxin analysis, targeted LC–MS/MS, LC–HRMS, ELISA, and PPIA were combined within a single workflow, showing that effect-based assays often captured broader cumulative toxicity than congener-specific quantification alone [109]. Compared with purely structure-driven SS/NTS, such hybrid strategies better support toxicological completeness and mixture-level interpretation.

 doi:10.20944/preprints202604.0384.v1

Large-scale sludge screening further illustrates the scalability of HRMS for solid matrices. A Swiss nationwide sludge survey combined multi-extraction strategies with Orbitrap-based LC–HRMS and used homologous-series logic and Kendrick mass defect analysis to expand the annotation of surfactants and PFAS beyond library-confirmed compounds. Compared with water-based screening, these sludge workflows are more oriented toward integrative exposure assessment, mass-load estimation, and transformation dynamics during anaerobic digestion [27].

Algorithmic refinement is also becoming central to transformation-product discovery. Entropy similarity–driven transformation reaction molecular networking (ESTRMN) integrates LC–Orbitrap data with entropy-based spectral similarity scoring and transformation knowledge-guided prediction to resolve parent–product relationships in wastewater. Compared with broad multiclass suspect screening or CCS-supported PFAS workflows, this strategy is more explicitly reaction-aware and aims to improve mechanistic interpretation of TP formation [26].

A similar class-oriented advance has been demonstrated for ladder polyether marine toxins, where fragmentation-rule–based screening of HRMS/MS data exploited sequential dehydration and desulfation patterns together with family-specific diagnostic fragments to classify polyether-like features prior to database matching [132]. Compared with conventional library-dependent NTS, such rule-based workflows enable faster class-specific toxin discovery, although unambiguous distinction of structural isomers still requires orthogonal evidence.

Despite these advances, identification confidence in SS/NTS workflows remains strongly dependent on spectral-library completeness, high-quality MS/MS reference spectra, and transparent reporting of acquisition parameters and tolerance criteria.

Overall, SS and NTS workflows substantially expand analytical coverage beyond conventional target lists by enabling the discovery of previously unmonitored compounds, transformation products, and mixture patterns across water, biota, sludge, and consumer-product matrices. Their main strengths lie in chemical-space expansion, retrospective data interrogation, and increasingly refined prioritization through CCS support, molecular networking, reactivity-directed screening, and bioassay integration. However, these advantages remain constrained by annotation uncertainty and limited reference-standard availability, making harmonized confidence assignment essential for translating expanded feature detection into reproducible and risk-relevant environmental interpretation.

Table S1 comparatively summarizes the principal analytical configurations currently applied to molecular ECs, including targeted LC–MS/MS, multidimensional LC–IMS–HRMS, and suspect/non-target screening workflows, with emphasis on instrumentation, analytical performance, identification capability, major strengths, and key methodological limitations.

5. Analytical Strategies for Particulate Emerging Contaminants (Microplastics)

Spectroscopic and Thermal–Mass-Based Techniques

Spectroscopic techniques remain central to microplastic (MP) analysis because they preserve particle-level information, including size, shape, and polymer identity. Their main strength is therefore not only polymer assignment, but also morphological characterization, which is essential for interpreting transport, weathering, and potential biological interactions. Recent developments increasingly combine imaging with vibrational spectroscopy to extend analysis toward smaller particles. For example, nanoplastics released during repeated uncapping and recapping of plastic water bottles were characterized by SEM, single-particle extinction and scattering (SPES), and μ-Raman spectroscopy, revealing releases on the order of a few tenths of ng per opening/closing event and particles dominated by amorphous polyethylene, likely derived from cap abrasion. Similarly, in tap-water monitoring, direct collection on 25 μm stainless-steel filters followed by micro-IR spectroscopy enabled particle-resolved identification, with mean concentrations of 12.5 MPs m^{-3} and 32.2 anthropogenic particles m^{-3}; the dominant polymers were polyamide, polyester, and polypropylene, with a lower contribution from poly(lactic acid) [60]. Despite these strengths,

 doi:10.20944/preprints202604.0384.v1

vibrational methods remain limited for the lower nanoplastic range by size-dependent detectability, spectral interferences, and relatively low throughput.

Because the information delivered by MP methods is inherently complementary, no single platform currently provides complete characterization across all particle-size classes, polymer types, and environmental matrices. Imaging and vibrational spectroscopy provide particle-resolved information, whereas thermal and mass-based methods provide polymer-specific bulk quantification. A comparative overview of these complementary analytical windows is presented in Figure 2.

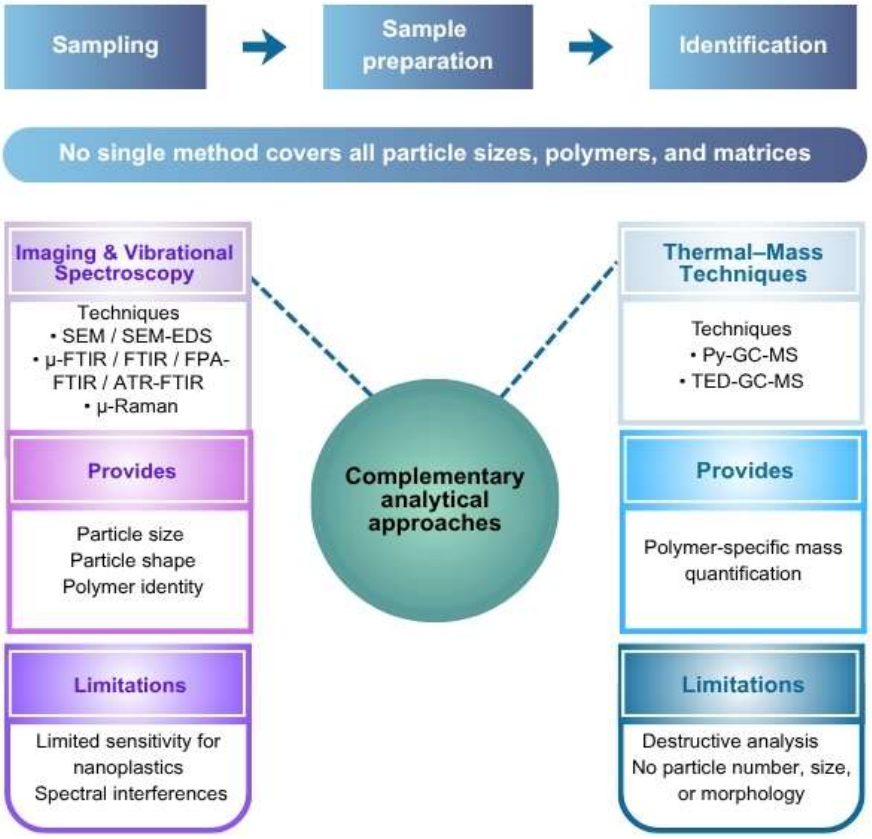

Figure 2. Complementary analytical approaches for microplastic characterization.

Thermal and mass-based methods, particularly pyr–GC–MS and related thermal–MS workflows, complement spectroscopic techniques by providing destructive but polymer-specific mass quantification. In contrast to vibrational methods, which emphasize particle counts and morphology, pyrolysis–GC–MS identifies polymers through characteristic degradation products and is therefore especially useful for nanoplastics, highly weathered particles, and optically ambiguous materials such as tire wear particles (TWPs). In urban stormwater, coupling particle counting with confirmatory thermal/MS enabled more robust characterization of TWPs: outlet concentrations after treatment were 1.8–32 MPs L^{-1}, including 1.3–32 TWPs L^{-1}, corresponding to 0.2–1.1 mg L^{-1} TWPs [90]. In aqueous matrices, ultrafiltration combined with H_2O_2 digestion before pyr–GC–MS enabled quantification of six polymers (PVC, PMMA, PP, PS, PE, PET), with linear calibration ($R^2 \geq 0.98$) and total nanoplastic concentrations up to 0.79 μg L^{-1} in surface water and 0.20 μg L^{-1} in groundwater [133]. Thermal/MS has also been extended to biodegradable polymers: pressurized liquid extraction followed by pyrolysis enabled quantification of PLA, PHA, PBS, PCL, and PBAT with recoveries of 74–116% and LOQs of 0.02–0.05 mg g^{-1} [134]. In soils, sediments, and sludge, recoveries of 79.6–91.4% were reported for PS, PE, PP, PMMA, PVC, and PET, with detection limits of 2.3–29.2 μg g^{-1} and total

 doi:10.20944/preprints202604.0384.v1

environmental concentrations of 4.6–51.4 μg g^{-1} [135]. Sensitivity has been further improved by coupling pyrolysis to triple-quadrupole MS in dynamic MRM mode, allowing quantification of twelve polymers at nanogram levels, with polymer-specific LODs as low as 1 ng and concentrations ranging from 2–35 μg L^{-1} in surface waters, 6.9–185.9 μg g^{-1} (dw) in sediments, and 0.1–13.3 mg g^{-1} (dw) in biota [136].

Overall, spectroscopic and thermal–mass-based methods should be regarded as complementary rather than competing strategies. Spectroscopic workflows provide particle-resolved identity and morphology, whereas thermal methods provide polymer-resolved bulk mass independent of optical detectability. Because thermal methods are destructive and do not preserve particle number, size, or shape, they are best applied as orthogonal mass-based tools alongside vibrational imaging when robust interpretation requires reconciliation of particle abundance with polymer load.

Table 1 comparatively summarizes the principal analytical strategies currently applied to particulate emerging contaminants (microplastics), highlighting their instrumentation, analytical outputs, main strengths, and key limitations.

Table 1. Analytical strategies for particulate emerging contaminants (microplastics) in water matrices.

Analytical strategy	Operational size range	Polymer identification	Quantification capability	Additional information obtained	Main strengths	Main limitations	Reference
Agglomeration with alkylated Fe_3O_4 + membrane filtration + Pyr-GC/MS	Nanoplastics; validated down to 20 nm for PS	PS and PMMA via characteristic pyrolysis products	Detection limits 0.02–0.03 μg L^{-1} for PS and PMMA; environmental PS detected in 11/15 samples at <0.07–0.73 μg L^{-1}	Polymer-specific mass concentrations in environmental waters	Very low detection limits; efficient nanoplastic enrichment; magnetic agglomeration reduces filtration resistance	Destructive; no particle-size, shape, or count information; validated for limited polymer scope	[133]
Pressurized liquid extraction (PLE) + thermochemolysis (TMAH) + Pyr-GC/MS	Mass-based MP fraction (<5 mm); no particle-size resolution; applicable to biodegradable polymers and nanoplastic-containing extracts	PLA, PCL, PBS, PBAT, and PHAs	Recoveries 74–116%; LOQs 0.02–0.05 mg g^{-1}; MDLs 0.06–0.17 μg $injection^{-1}$; calibration $R \geq 0.95$	Polymer-specific mass quantification with internal-standard correction	Simultaneous identification and quantification; suitable for complex matrices; thermochemolysis improves specificity	Destructive; no particle-number or morphology information; requires extraction and derivatization steps	[134]
TMAH digestion + dichloromethane dissolution + Pyr-GC/MS for solid matrices	Small MPs/NPs <150 μm; validated down to 50 nm for PS and PMMA	PS, PMMA, PE, PP, PVC, PET	Recoveries 79.6–91.4%; size-dependent recoveries 69–101%; LODs 2.3–29.2 μg g^{-1}; linearity $R^2 \geq 0.97$	Polymer-specific mass concentrations in soil, sediment, and sludge; total MNP levels 4.6–51.4 μg g^{-1} in real samples	Efficient extraction of small particles embedded in solid matrices; limited size effect; suitable for NOM-rich samples	Destructive; possible PVC-related benzene interference; centrifugation may cause minor nanoparticle losses	[135]

 doi:10.20944/preprints202604.0384.v1

Pyr-GC-QqQ-MS in dynamic MRM mode with internal-standard calibration	Mass-based MP fraction (<5 mm); operational water fraction typically >5 µm after filtration; also applicable to nanoplastic-containing fractions	Twelve polymers including PMMA, PP, PVC, PA, PC, PA66, PE, PET, ABS, SBR, PUR, and PS	Nanogram-level sensitivity (1–126 ng depending on polymer); example LODs: 1 ng for PA, PUR, and PS; 7 ng for PET; 10 ng for PC; 12 ng for PP; 60 ng for PE	Polymer concentrations reported in multiple matrices: 2–35 µg L^{-1} in surface waters, 6.9–185.9 µg g^{-1} dw in sediments, and 0.1–13.3 mg g^{-1} dw in biota	Very high sensitivity and selectivity; internal-standard calibration; suitable for multiple matrices; $CaCO_3$-assisted pyrolysis improves signal intensity	Destructive; no particle-number, size, or morphology information; requires specialized pyrolyzer–triple quadrupole instrumentation	[136]
Stormwater workflow combining filtration, FTIR, and Pyr-GC/MS for MPs and TWPs	Operational fraction >25 µm	FTIR: PET and PP; Pyr-GC/MS: poly(butadiene) rubber and styrene–butadiene rubber (SBR) for TWPs	Inlet concentrations 3.8–59 MPs L^{-1} and 2.5–58 TWPs L^{-1} (0.4–4 mg L^{-1} TWPs); outlet concentrations 1.8–32 MPs L^{-1} and 1.3–32 TWPs L^{-1} (0.2–1.1 mg L^{-1} TWPs); removal 35–88%	Fragments dominated the MP profile (>94%); ~92% of fragments were black rubbery TWPs confirmed by Pyr-GC/MS; supports treatment-performance assessment	Combines particle counting with chemical confirmation; explicitly captures dense TWPs often missed by optical methods alone; directly useful for stormwater treatment benchmarking	Misses smaller MPs and NPs because of size cut-off; Pyr-GC/MS is destructive and increases analytical cost/time; FTIR is limited for black rubber; mass estimates remain method-dependent	[90]

MPs, microplastics; NPs, nanoplastics; TWPs, tire-wear particles; Pyr-GC/MS, pyrolysis–gas chromatography/mass spectrometry; FTIR, Fourier-transform infrared spectroscopy; TMAH, tetramethylammonium hydroxide; PS, polystyrene; PMMA, poly(methyl methacrylate); PE, polyethylene; PP, polypropylene; PVC, poly(vinyl chloride); PET, polyethylene terephthalate; PLA, polylactic acid; PCL, polycaprolactone; PBS, poly(butylene succinate); PBAT, poly(butylene adipate-co-terephthalate); PHAs, polyhydroxyalkanoates; PA, polyamide; PA66, polyamide 66; PC, polycarbonate; ABS, acrylonitrile butadiene styrene; SBR, styrene–butadiene rubber; PUR, polyurethane; NOM, natural organic matter; MRM, multiple reaction monitoring; LOD, limit of detection; LOQ, limit of quantification; MDL, method detection limit; dw, dry weight.

6. Environmental and Human Health Risk Assessment

6.1. Environmental Risks of Molecular Emerging Contaminants

Environmental risks of molecular emerging contaminants are governed not only by their occurrence in water systems, but also by transformation processes, chronic emission pathways, bioavailability, and species-specific sensitivity. In many cases, treatment or environmental transformation does not eliminate risk, but instead reshapes it through the formation of more reactive, toxic, or persistent products. Accordingly, risk assessment must integrate parent compounds, transformation products, transmissible biological hazards, and matrix-dependent exposure conditions.

Transformation processes can modify the persistence and hazard of halogenated emerging contaminants, although confirmed examples of enzymatic C–F bond cleavage remain rare. Mechanistic evidence was provided for the histidyl-ligated heme enzyme LmbB2, which catalyzed

 doi:10.20944/preprints202604.0384.v1

C–H and C–F bond activation during hydroxylation of halogenated L-tyrosine analogues. Defluorination of 3-fluoro-L-tyrosine was confirmed by ^19F-NMR detection of released fluoride [137]. Although these substrates were model aromatic fluorinated compounds rather than environmental PFAS, the study provides proof of principle that biocatalytic oxidation can, under specific conditions, induce C–F bond cleavage. From an environmental-risk perspective, this suggests that transformation pathways for some fluorinated contaminants may exist, although their real environmental relevance remains uncertain.

At the life-cycle scale, however, PFAS risk remains dominated by persistence and sustained emissions rather than demonstrated environmental degradation. Scenario projections indicate that legacy PFAAs may still account for about 3.64 × 10^4 kg by 2050, while emerging PFAS subclasses are expected to represent an increasing share of total emissions [79]. This shift implies that substitution may alter PFAS composition without proportionally reducing the total fluorinated burden entering the environment. In parallel, fluoropolymer-related risk cannot be assessed only from the relative inertness of the final polymer, because the major environmental burden occurs upstream during production, where diverse fluorinated by-products and non-gaseous PFAS are released to air and water and remain incompletely characterized [138]. Together, these findings indicate that long-term PFAS risk is shaped not only by intrinsic persistence, but also by incomplete emission reporting and continuing substitution toward less-characterized fluorinated chemistries.

WWTPs further reinforce this chronic exposure pattern by acting as continuous PFAS release pathways. A U.S. meta-analysis showed that biological treatment increased effluent PFOA by 6.0 ± 1.6 ng L^{-1}, consistent with precursor biotransformation, whereas PFOS showed no significant net change. Despite an annual decline of about 13% between 1999 and 2020, mean effluent PFOA still remained 8.4 ± 0.4 ng L^{-1} during 2013–2020, corresponding to an estimated 383 ± 20 kg yr^{-1} discharged to U.S. surface waters [80]. Thus, even low ng L^{-1} effluent concentrations can generate substantial cumulative loading, confirming WWTPs as persistent contributors to PFAS exposure.

A similarly widespread exposure pattern has been reported for psychopharmaceuticals and illicit drugs, which represent another class of bioactive molecular ECs. A global meta-analysis compiling 331 concentration records from 108 studies across 100 countries showed widespread occurrence of these compounds in surface waters, from pg L^{-1} to μg L^{-1} levels. Among the highest reported concentrations, caffeine reached 41.82 μg L^{-1}, methamphetamine 9.70 μg L^{-1}, benzoylecgonine 8.03 μg L^{-1}, and cocaine 2.89 μg L^{-1} [139]. Ecological risk analysis further suggested that compounds such as MDA, Δ^9-THC, and 11-hydroxy-THC may pose comparatively higher risks to aquatic organisms, especially in regions with limited wastewater treatment. These findings broaden the environmental risk picture beyond PFAS by showing that persistent exposure also arises from continuously consumed bioactive contaminants with high biological potency.

Beyond occurrence alone, photochemical transformation is a major process controlling the persistence and hazard of psychotropic drugs in sunlit waters, but its importance is strongly matrix-dependent. A recent synthesis showed that both direct and indirect photolysis can contribute across antidepressants, antiepileptics, antipsychotics, and illicit drugs, with DOM, nitrate, and pH acting as key controls. In realistic matrices, phototransformation may be markedly enhanced; for example, cocaine decreased by 90% after 20 h under natural solar irradiation in synthetic municipal wastewater effluent, whereas only ~22% transformation occurred after 60 h in distilled water. By contrast, high DOM can suppress photolysis through light screening, with 67 mg C L^{-1} reducing direct and indirect transformation rates by ~84%. Importantly, transformation does not necessarily reduce risk: carbamazepine photolysis produced 10,11-epoxycarbamazepine (~25%) and acridine (~10%) after 8 h, the latter being more toxic than the parent compound [20]. Thus, as for PFAS, persistence alone is insufficient for risk evaluation because matrix conditions can either accelerate attenuation or prolong pseudo-persistence while simultaneously generating more hazardous products.

Beyond chemical transformation, ARGs introduce a distinct environmental risk dimension because they behave as transmissible genetic pollutants rather than conventional toxicants. Municipal landfill refuse has been identified as a hotspot of multidrug resistance genes, which were

 doi:10.20944/preprints202604.0384.v1

the dominant ARG class and were strongly associated with mobile genetic elements, metal resistance genes, and potential pathogenic hosts [40]. This co-occurrence supports co-selection and enhanced horizontal gene transfer in heterogeneous landfill environments, suggesting that landfill-derived ARGs may spread through leachate, bioaerosols, and downstream water systems. In contrast to molecular ECs, whose risk is driven mainly by persistence and toxicity, ARGs can undergo ecological amplification, underscoring the need to integrate biological and chemical monitoring within environmental risk assessment.

This transmissible risk is further intensified under mixture exposure. Hayes et al. showed that ciprofloxacin alone increased the class-1 integron integrase gene intI1 at 40 μg L^{-1}, whereas co-exposure with diclofenac (50 μg L^{-1}), metformin (26 μg L^{-1}), or 17-β-estradiol (24.4–24.8 μg L^{-1}) produced significant increases already at 10 μg L^{-1} ciprofloxacin, and at 20 μg L^{-1} in all mixtures [33]. These findings indicate that non-antibiotic pharmaceuticals can lower AMR selection thresholds to concentrations more typical of impacted waters, making ARG-related risk more complex than single-compound assessment would suggest. At the global scale, this risk is amplified where high antibiotic emissions coincide with limited wastewater treatment and low dilution capacity, particularly in densely populated regions of South and Southeast Asia [44]. Together, these results highlight untreated or insufficiently treated wastewater as a major pathway linking antibiotic consumption to environmental AMR selection pressure.

Engineered carbon nanomaterials represent another distinct class of molecular ECs whose risks extend beyond intrinsic toxicity to include vector and mixture-modulating effects. Under estuarine microcosm conditions, fullerene soot, multiwall carbon nanotubes, and graphene underwent aggregation and surface transformation that altered biological responses. Fullerene soot showed moderate intrinsic toxicity toward Vibrio fischeri (EC_{50} ≈ 26 mg L^{-1}), whereas Daphnia magna was generally more sensitive. In binary mixtures with organic contaminants such as malathion, diuron, glyphosate, and triclosan, interactions were mostly antagonistic, although synergistic effects were observed in some cases, notably malathion–fullerene soot toward D. magna [140]. Smaller aggregates were more toxic because of higher surface reactivity and bioavailability, and the nanomaterials also acted as vectors for co-contaminants, modifying internal exposure. Accordingly, nanomaterials should be considered not only as toxicants themselves, but also as modifiers of contaminant fate and mixture toxicity.

Transformation-dependent risk is also evident for disinfection by-products. Comparative experiments with chlorine, chloramine, and ozone showed that disinfectant identity governs not only DBP yield but also DBP class distribution, including trihalomethanes, haloacetic acids, haloacetonitriles, halonitromethanes, haloacetamides, haloacetaldehydes, haloketones, and halobenzoquinones. Chlorination favored carbonaceous DBPs through electrophilic substitution, chloramination promoted nitrogenous DBPs through reactive nitrogen incorporation, and ozonation enhanced oxidative fragmentation and quinone-type product formation [141]. Thus, disinfectant choice reshapes DBP chemical space and downstream toxicological profiles rather than simply changing overall concentrations. Consistent with this, bisphenol analogue chlorination produced highly reactive non-traditional carbonyl DBPs such as 2-butene-1,4-dial (BDA) and related BDAs, with formation favored under neutral conditions and suppressed during chloramination [114]. These findings reinforce that environmental risk assessment must consider not only parent compounds, but also treatment-driven transformation pathways that generate structurally distinct and sometimes more reactive products.

A similar concern applies to UV–chlor(am)ine treatment, where improved contaminant removal may coincide with the formation of more bioactive transformation products. Using acesulfame as a model sweetener, monochloramine alone caused no measurable degradation within 30 min, whereas UV photolysis removed 92% (k = 0.086 min^{-1}) and UV/NH_2Cl further increased the rate to 0.115 min^{-1} under the same conditions [113]. HRMS showed that reactive chlorine species generated chlorinated transformation products absent in UV-only systems, and Vibrio fischeri assays indicated increased toxicity after UV/NH_2Cl treatment, with chlorinated halo-alcohol products identified as major

 doi:10.20944/preprints202604.0384.v1

contributors [113]. A comparable pattern was reported for sucralose, whose acute toxicity increased markedly after UV-driven transformation, with EC_{50} decreasing from 2670 to 156.2 mg L^{-1} in Microtox assays [53]. Together, these results show that treatment-driven transformation can reduce parent-compound concentrations while increasing mixture toxicity, reinforcing the need to include transformation products in advanced treatment and reuse risk assessment.

Rubber-derived transformation products provide one of the clearest examples of such risk amplification. Tire-wear particle leachates containing 6PPD-quinone caused rapid adult coho salmon mortality, with 25–50% mortality within 24 h even at the lowest nominal leachate concentration (100 mg L^{-1}), and complete mortality at 320 and 1000 mg L^{-1}. Under the same 320 mg L^{-1} exposure, however, adult chum salmon survived, demonstrating pronounced interspecies variability [142]. This taxon dependence is consistent with broader toxicity data, where reported LC_{50} values ranged from 0.50–1.00 μg L^{-1} for salmonids such as lake trout, brook trout, and rainbow trout, but increased to 162.2 μg L^{-1} for Gobiocypris rarus and 500 μg L^{-1} for red drum, while arctic char and sturgeons showed no mortality at 14.2 μg L^{-1} [69]. These findings indicate that 6PPD-quinone can drive acute ecological impacts at environmentally relevant concentrations, but that hazard is strongly species-dependent.

Sublethal effects also remain important under chemically dynamic natural conditions. In a 21-day exposure of Corbicula fluminea, both 6PPD and 6PPDQ showed minimal degradation, yet induced DOM humification and shifts toward more recalcitrant organic matter. Despite this apparent "aging" of the matrix, toxicity remained evident, including AChE inhibition, CAT and GSH-Px induction, increased LDH, and ecologically relevant behavioral impairment, with stronger disruption under 6PPDQ [107]. Thus, DOM transformation should not automatically be interpreted as a protective process, since matrix aging may coexist with persistent biological stress.

In addition to lethality and sublethal toxicity, rubber-derived transformation products may exert endocrine effects. Effect-directed analysis identified 4-hydroxydiphenylamine (4HDPA), a hydrolysis product of PPD antiozonants, as the major estrogenic driver in elastomer leachates, with EC_{10} and EC_{50} values of 330 ± 59 and 820 ± 180 μg L^{-1}, respectively, in the YES assay. Under assay conditions, its redox partner QMI was almost completely converted to 4HDPA, and measured leachate concentrations fully explained the observed estrogenic activity. Environmental screening further detected 4HDPA at ng L^{-1} to low μg L^{-1} levels in rivers and in a rubber dam [143]. Compared with the acute salmonid toxicity of 6PPD-quinone, these findings broaden the hazard profile of rubber additives by showing that transformation can also yield endocrine-active products.

Plastic-derived consumer products represent another overlooked source of molecular EC risk. Cigarette filters, composed mainly of cellulose acetate fibers and adhesive additives, contained total phthalate concentrations ranging from 391.23 to 132,216.69 ng g^{-1}, with DBEP, DBP, and DEEP accounting for more than 45% of the total burden. Estimated smoker exposure ranged from 30.99 to 10,472.61 ng kg^{-1} bw day^{-1}, and carcinogenic risk estimates exceeded the 10^{-6} benchmark [144]. Although this pathway differs from aquatic exposure scenarios, it highlights how plastic-associated additives can contribute both to direct human exposure and to broader environmental release.

At the management scale, the magnitude of tire-derived emissions supports treating these contaminants as a global pollution issue rather than a localized runoff problem. Global tire production reached 23 million tonnes in 2024, and wear-related losses correspond to estimated tire-wear particle emissions of 1.12 million tonnes yr^{-1} in the United States and 1.327 million tonnes yr^{-1} in the European Union. Because additives and fillers account for about 16–17% of tire mass, this represents a dispersed chemical load of roughly 185,000 tonnes yr^{-1} and 225,000 tonnes yr^{-1}, respectively. In response, a management framework for tire additive pollution has been proposed that emphasizes safer alternatives, life-cycle assessment, transparency in tire composition, rigorous effects characterization, and international harmonization [145]. Upstream reformulation strategies, including bio-based elastomers, regenerated carbon black, rice-husk-derived silica, recycled polystyrene, and vegetable-oil plasticizers, may also reduce future emissions; however, their effects on additive release and transformation-product formation remain poorly characterized [146].

 doi:10.20944/preprints202604.0384.v1

Together, these findings indicate that effective mitigation will require both downstream control and upstream redesign to avoid regrettable substitution.

Although this subsection focuses on molecular ECs, particulate contaminants can also modify the environmental risk profile of co-occurring chemicals. Micro- and nanoplastics (MNPs) can alter aquatic biogeochemical processes and contaminant behavior. A recent synthesis showed that MNPs interfere with carbon, nitrogen, sulfur, and phosphorus cycling by altering microbial community structure, enzyme activity, and redox microenvironments. In addition, plastisphere biofilms can act as reservoirs for pathogens and ARGs, thereby enhancing horizontal gene transfer and ecological persistence. MNPs also interact synergistically with other emerging contaminants through adsorption, hydrophobic partitioning, and electrostatic interactions, which may increase contaminant bioavailability and toxicity [34]. Thus, unlike conventional particulate carriers, MNPs function as active ecological modifiers that can indirectly amplify contaminant risks and water-security concerns.

For engineered nanomaterials, recent work has further shown that environmental risk cannot be assessed from environmental occurrence alone. A USEtox-based life-cycle assessment of carbon nanotubes indicated that aquatic ecotoxicity associated with production processes could equal or exceed impacts from modeled environmental CNT releases, with production-stage burdens largely driven by metal emissions from electricity generation [147]. This upstream perspective contrasts with monitoring-based studies focused only on post-release concentrations, and suggests that dominant ecotoxic impacts may arise before nanomaterials even enter aquatic systems. Accordingly, nanomaterial risk assessment should integrate emission inventories, fate processes, and ecotoxicity characterization within a life-cycle framework rather than relying solely on measured environmental concentrations.

Region-specific nanoscale fate modeling also highlights how strongly nanomaterial risk differs from that of dissolved contaminants. For copper nanoparticles, a freshwater USEtox-based model incorporating dissolution, aggregation, pseudosedimentation, advection, and resuspension produced characterization factors ranging from 3.87 × 10^3 to 11.11 × 10^3 CTUe across 17 subcontinental regions, with Africa identified as the most sensitive region. Sensitivity analysis showed that freshwater depth, particle radius, suspended solids, and dissolution rate were major drivers of risk estimates [148]. In contrast to conventional molecular ECs, whose fate is often approximated by partition coefficients and degradation rates, nano-Cu behavior is strongly governed by aggregation and sediment–water exchange, underscoring the need for nanospecific fate models.

Mechanistic studies further confirm that the hazard profile of engineered nanomaterials is dynamically shaped by water chemistry. Nano-Cu, nano-CuO, and $Cu(OH)_2$ showed distinct aggregation, sedimentation, dissolution, and redox-transformation behavior across natural waters differing in ionic strength, pH, and organic content. Nano-Cu and $Cu(OH)_2$ rapidly formed micrometer-scale aggregates, whereas nano-CuO remained comparatively more stable; however, aggregation did not directly predict sedimentation, indicating separate control by density, oxidation state, and surface chemistry. Dissolution increased under acidic conditions, while saline waters promoted insoluble chloride and carbonate phases. Even low phosphate concentrations altered surface charge and stabilized nano-CuO suspensions [149]. These findings demonstrate that nanomaterial mobility and hazard are not fixed intrinsic properties, but depend strongly on environmental geochemistry.

More broadly, a critical evaluation of engineered nanomaterial ecotoxicology emphasized that hazard testing is still often performed at concentrations exceeding realistic environmental levels, with insufficient consideration of aging, heteroaggregation, transformation, and realistic compartment partitioning. In addition, ENMs may act through both particulate and dissolved ionic forms, making dose metrics more complex than for conventional molecular ECs. Compared with PFAS or DBPs, where risk assessment is increasingly driven by concentration and structure, nanomaterial risk requires scenario-based evaluation that explicitly integrates exposure modeling, transformation dynamics, and body-burden considerations [150]. Overall, the evidence discussed in this section

 doi:10.20944/preprints202604.0384.v1

indicates that environmental risks of molecular ECs arise from a combination of persistence, continuous release, transformation, and indirect ecological effects rather than from parent-compound concentrations alone. This supports a shift from occurrence-based assessment toward integrated frameworks that combine exposure, transformation, bioactivity, and long-term emission context.

6.2. Human Health Risks

Human exposure to emerging contaminants occurs through multiple environmental pathways, including drinking water, food consumption, airborne particles, and indirect transfer through environmental matrices. In addition to direct exposure to parent compounds, transformation products, particulate carriers, and complex contaminant mixtures can substantially modify exposure dynamics and toxicological outcomes. Consequently, human-health risk assessment increasingly requires integrated evaluation of chemical, biological, and environmental processes that influence contaminant mobility, bioavailability, and cumulative exposure.

Human-health risks from emerging contaminants increasingly arise through indirect and combined exposure pathways rather than from single contaminants in isolation. Micro- and nanoplastics are one example, because they can transport pathogens, antibiotic-resistant bacteria, resistance genes, and sorbed chemicals through biofilm formation and food-web transfer, thereby linking microbial and chemical exposure routes relevant to drinking water and seafood safety [34]. Chemical transfer through aquatic food webs is already evident for PFAS: in Portuguese commercial fish and bivalves, HRMS screening followed by targeted analysis showed that several samples exceeded EU maximum levels for PFOA under Regulation (EU) 2023/915, demonstrating that environmental contamination can translate directly into dietary exposure [96]. More broadly, recent syntheses indicate that soil health strongly influences whether biosolids- or wastewater-amended soils behave as sinks or secondary sources of micropollutants to groundwater and surface waters, reinforcing the need for integrated soil–water risk assessment in reuse systems [51].

MPs may also amplify toxin exposure by acting as concentration vectors for cyanotoxins. Adsorption studies showed up to 28-fold enrichment of microcystins on polymer surfaces, with maximum levels reaching 156 μg g^{-1} for the more hydrophobic congener MC-LF on polystyrene. Sorption was congener-dependent (MC-LF > MC-LR), polymer-specific (PS > PE > PVC > PET), and stronger for smaller particles, indicating dominant control by hydrophobic partitioning [35]. Because adsorption remained significant across pH 5–9, including bloom-impacted waters, these findings suggest that risk assessment based only on dissolved MC-LR may underestimate exposure, especially when particulate-bound fractions facilitate trophic transfer or create local hotspots.

This concern extends to water treatment, where contaminant removal does not necessarily equate to detoxification. For cyanotoxins, ozonation, chlorination, UV-based oxidation, and permanganate treatment show distinct kinetics, but structural degradation may still generate reactive intermediates, including halogenated products or aldehydic fragments from cleavage of toxic moieties such as the Adda group in microcystin-LR [151]. A related issue arises from nitrosamine precursor formation in biologically active waters. Controlled incubation experiments showed that microbial degradation of nitrogenous substrates increased NDMA formation potential by 2.6–7.9-fold before subsequent biodegradation reduced it again, with low-molecular-weight extracellular fractions (<1 kDa) dominating the precursor pool [152]. Because commonly monitored amines accounted for only a minor fraction, these results indicate that routine monitoring may miss

 doi:10.20944/preprints202604.0384.v1

biologically generated precursor reservoirs that become toxicologically relevant only after chloramination. Together, these findings show that process-dependent transformation can shift, rather than eliminate, human-health risk during drinking water treatment.

Low-level pollution may also indirectly elevate human exposure by stimulating harmful cyanobacterial blooms. A recent synthesis reported a mean 57.9% increase in microcystin production under sub-toxic contaminant exposure, with most stimulatory responses occurring at ≤100 μg L^{-1} and many at ≤0.6 μg L^{-1}. Antibiotics accounted for most documented cases, and stimulation was linked to the up-regulation of toxin biosynthesis and transport genes [153]. Thus, contaminants present below conventional toxicological thresholds may still enhance toxin burdens in source waters, increasing indirect human exposure through drinking water supplies.

Direct human exposure to cyanotoxins is not limited to drinking water. Commercial algal dietary supplements have been reported to contain microcystins up to 60 μg g^{-1}, corresponding to estimated daily intakes up to 75-fold above the tolerable daily intake of 0.04 μg kg^{-1} body weight [109]. More broadly, chronic low-dose exposure may represent a more pervasive risk than episodic exceedances. Although WHO guidance values are based mainly on microcystin-LR, environmental matrices frequently contain mixtures of microcystins, cylindrospermopsin, anatoxin-a, and nodularin, as well as modified congeners whose toxic equivalency remains poorly defined [57]. Because routine monitoring still focuses on a limited subset of toxins, total cyanotoxin burden and mixture toxicity may be systematically underestimated across drinking water, food webs, and irrigation-related exposure pathways.

A similar structural undercoverage affects disinfection by-products. Large HRMS compilations list thousands of DBP structures, but only a minority have been confirmed with standards, indicating that exposure assessment remains biased toward analytically accessible compounds [4]. This gap becomes critical when highly toxic but previously unrecognized DBPs are formed. Recent GC–HRMS studies identified six alicyclic HCPDs in chlorinated and chloraminated drinking water, five of them newly reported as DBPs; one compound, 1,2,3,4,5,5-hexachloro-1,3-cyclopentadiene, showed in vivo toxicity values orders of magnitude higher than regulated THMs and HAAs and predicted bioconcentration factors of 384–3980 [18]. Even for regulated DBPs, population-scale risks remain measurable: a global THM synthesis reported a weighted mean concentration of 26.74 μg L^{-1} and an average lifetime cancer risk of 6.45×10^{-5}, with a quantifiable contribution to bladder-cancer burden and marked regional disparities [154]. Thus, both regulated and unresolved DBP fractions remain relevant for long-term health risk in drinking water systems.

Emerging evidence also links non-classical contaminants to endocrine-related developmental outcomes. In a Chinese birth cohort, each doubling of early-pregnancy urinary 2-hydroxy-benzothiazole was associated with lower childhood BMI at age two, while tolyl-triazole and 2-hydroxy-benzothiazole were associated with reduced maternal free thyroxine and increased neonatal TSH. Mediation analysis further supported thyroid disruption as a mechanistic pathway [155]. These findings extend the human-health risk picture beyond conventional carcinogenic or acute-toxic endpoints and indicate that low-level chronic exposure to traffic- and consumer-product-derived contaminants may also affect endocrine and developmental health.

Overall, these findings demonstrate that human-health risks associated with emerging contaminants arise from a complex interplay of environmental transport, transformation processes,

 doi:10.20944/preprints202604.0384.v1

particulate vectors, and mixture effects rather than from individual parent compounds alone. This complexity highlights the limitations of monitoring strategies focused on a restricted number of regulated analytes and supports the development of integrated analytical and risk-assessment frameworks that incorporate transformation products, particulate-bound fractions, and multi-class contaminant mixtures across drinking water and food-exposure pathways.

6.3. Risks Associated with Microplastics

Microplastic risk extends beyond simple particle occurrence alone and increasingly involves interactions with biological barriers, ecosystem processes, and co-occurring contaminants. Accordingly, risk assessment should address not only physical particle effects, but also vector functions, indirect ecological disruption, and transfer between aquatic and terrestrial compartments.

A recent One Health review further emphasized that micro- and nanoplastics should be considered persistent low-dose stressors across the lifespan, as growing evidence links their exposure to oxidative stress, inflammation, mitochondrial dysfunction, and cellular senescence, with potentially greater consequences in aging populations because of cumulative exposure and reduced physiological resilience [156].

Recent evidence has broadened concern beyond gastrointestinal and pulmonary exposure to include potential neurotoxicity of textile-derived micro- and nanoplastics. Fibrous particles released from synthetic textiles such as polyester, acrylic, nylon, and polyethylene have been detected in indoor air, household dust, and even human tissues, including brain samples [157]. Mechanistic studies suggest that nanoscale particles may reach the brain either through olfactory transport after inhalation or via systemic circulation and passage across the blood–brain barrier. Once internalized, they have been linked to oxidative stress, neuroinflammation, microglial activation, disruption of tight-junction proteins, and protein aggregation pathways associated with neurodegenerative disease [157]. These findings indicate that textile-derived MNPs should be considered not only as environmental particulates, but also as potential neurotoxic stressors.

At the ecosystem scale, MNPs also act as active modifiers of aquatic functioning rather than inert particles. Integrative analyses show that they interfere with carbon, nitrogen, sulfur, and phosphorus cycling by altering microbial community structure, enzyme activity, and redox microenvironments [34]. Such disturbances may impair nutrient sequestration, promote eutrophication, and reduce ecosystem resilience. In this sense, microplastic risk resembles that of other emerging contaminants, in that indirect ecological effects may be as important as direct toxicity.

Agricultural soils represent another important exposure compartment because of fragmentation of plastic mulching films. In a field study across Finland, Germany, and Spain, both conventional polyethylene mulch and biodegradable starch-blended PBAT mulch reduced microbial activities linked to soil functioning, particularly nitrogen cycling, with stronger effects after the second season, at higher loading (0.05% w/w), and in southern regions [158]. These results indicate that microplastic risks in soil depend on polymer type, exposure intensity, duration, and regional conditions, supporting the need for site-specific assessment.

MNPs also create biologically active plastisphere communities enriched in pathogens and antibiotic resistance genes. These biofilms can enhance microbial persistence and horizontal gene transfer, raising concern that microplastics may facilitate long-distance transport of microbial hazards

 doi:10.20944/preprints202604.0384.v1

and indirect exposure through drinking water and seafood pathways [34]. Compared with dissolved contaminants, microplastics therefore combine particulate, chemical, and microbiological risk dimensions within the same carrier.

Wastewater treatment may further shift these risks from water to land rather than removing them. A probabilistic risk assessment for sludge-amended soils derived an HC5 of 145 MPs kg^{-1} dw and suggested that microplastic contamination could affect 15–18% of soil species under realistic scenarios, compared with about 8% in control soils; under worst-case conditions, the potentially affected fraction rose to ~39% [32]. This indicates that apparent removal in WWTPs often represents redistribution to biosolids, reinforcing the need for regulatory thresholds for sludge intended for land application.

Overall, risks associated with microplastics arise not only from particle presence, but also from their capacity to cross biological barriers, disrupt ecosystem processes, host microbial hazards, and redistribute contamination between environmental compartments. These findings support integrated risk-assessment frameworks that combine particulate metrics with biofilm-related hazards, adsorption behavior, and land–water transfer processes rather than relying solely on occurrence data.

7. Knowledge Gaps, Analytical Challenges, and Future Perspectives

Despite major analytical progress, important gaps remain in the monitoring of emerging contaminants and microplastics across natural and engineered water systems. These limitations arise from shortcomings in sampling representativeness, matrix-adapted extraction, analytical harmonization, transformation-product coverage, and the conversion of occurrence data into risk-relevant interpretation. Addressing them will require integrated and standardized frameworks that link molecular and particulate contaminants across water, sludge, soil, and biota compartments.

A first critical gap concerns sampling design. For molecular ECs, event-driven pulses, seasonal variability, and precursor transformation can strongly alter measured concentrations, yet monitoring still often relies on sparse or single-timepoint sampling. Future strategies should combine event-triggered, composite, passive, and multi-season approaches to capture transient peaks, chronic background exposure, and spatial source variability across urban, agricultural, and reuse-impacted systems [16,70,80,93]. A comparable limitation applies to stormwater MPs and TWPs, for which no harmonized methodology yet permits robust benchmarking of gross-pollutant capture devices across size fractions and polymer types. Standardized protocols should therefore define minimum size cut-offs, QA/QC requirements, and dual reporting of particle counts together with polymer or TWP mass [90].

Sample preparation remains another major bottleneck. Although SPE, DLLME, MSPD, large-volume enrichment, and polymeric-resin extraction have expanded analyte coverage and improved sensitivity, no single preparation strategy is suitable for the full diversity of contaminants and matrices considered in this review [18,95,96]. Salinity, dissolved organic matter, lipids, particulates, and co-extracted interferences continue to influence recovery, matrix effects, and detection limits. Future work should therefore prioritize fit-for-purpose extraction, broader use of isotope-labeled standards, and transparent reporting of matrix-specific recoveries, blank contamination, and procedural losses, especially in multiclass HRMS investigations [106].

For molecular ECs, targeted LC-MS/MS and GC-MS remain indispensable for accurate quantification of priority compounds, but they cannot adequately cover the expanding space of

 doi:10.20944/preprints202604.0384.v1

transformation products, replacement PFAS, novel DBPs, and tire-derived quinones [22,23]. HRMS-based suspect and non-target screening has thus become essential, yet annotation confidence, spectral-library completeness, interlaboratory comparability, and regulatory translation remain major constraints. Progress will depend on harmonized confidence-level reporting, curated open-access spectral databases, fragmentation-guided screening, and stronger linkage between non-target discovery and subsequent targeted confirmation [24–27].

For MPs and nanoplastics, no single analytical platform yet provides comprehensive characterization across all relevant particle sizes, polymer classes, and matrices. Spectroscopic techniques preserve size, morphology, and polymer identity, whereas thermal and mass-based methods provide complementary polymer quantification, including for highly weathered or optically unresolved particles. However, interstudy comparability remains limited by inconsistent digestion methods, size thresholds, reporting units, confirmation criteria, and blank correction procedures. Future workflows should therefore adopt standardized multi-method strategies combining particle-resolved and mass-based data, with explicit reporting of minimum detectable size, recovery, instrumental limitations, and QA/QC across water, sludge, sediment, soil, and biota [29–31,103,135,136].

A further cross-cutting issue is that apparent removal does not necessarily indicate elimination. For MPs, removal from water often reflects transfer to sludge, sediments, or soils. For molecular ECs, treatment may generate transformation products or shift contaminant partitioning without reducing overall hazard. Monitoring frameworks should therefore evaluate redistribution, persistence, and transformation alongside parent-compound removal, especially in wastewater treatment and water-reuse systems where contaminants may recirculate across water-soil-plant-food pathways [18,19,29,32,37,47].

Finally, risk assessment remains limited by analytical methodology. Incomplete structural identification, partly due to the lack of commercially available standards, insufficient data on transformation products and mixture effects, poor harmonization across studies, and limited long-term exposure data continue to constrain robust environmental and human-health evaluation. Future priorities should therefore include harmonized sampling and analytical workflows, integration of targeted quantification with HRMS-enabled suspect and non-target screening, combined particle-count and polymer-mass approaches for MPs and TWPs, and closer integration of analytical chemistry with toxicology, bioavailability assessment, and exposure modeling [24,26,29,30,34,37].

Overall, future progress requires a shift from occurrence-based monitoring toward harmonized, matrix-aware, and risk-relevant analytical systems. Such frameworks will be essential for translating increasingly sophisticated analytical data into comparable evidence and effective regulatory action for emerging contaminants and microplastics in natural and treated waters.

8. Conclusions

This critical review demonstrates that the analysis of ECs and MPs in natural and treated waters can no longer rely on fragmented analytical approaches based on single techniques or isolated environmental compartments. The increasing diversity of molecular ECs—including pharmaceuticals, PFAS, disinfection by-products, pesticides, tire-derived chemicals, nanomaterials, and resistance-related contaminants—together with the physicochemical and morphological

 doi:10.20944/preprints202604.0384.v1

complexity of MPs, requires analytical frameworks capable of simultaneously addressing chemical diversity, particulate heterogeneity, and complex environmental matrices.

Across the reviewed literature, a central finding is that occurrence data alone do not adequately represent environmental risk. Episodic storm-driven peaks, treatment- and environment-induced transformation, matrix-dependent partitioning, and redistribution across water, sludge, sediments, soils, crops, and biota all shape exposure pathways and hazard. Analytical interpretation must therefore move beyond concentration reporting toward a more integrated understanding of contaminant fate, mixture composition, persistence, and transfer across interconnected compartments.

A major strength emerging from recent analytical developments is the complementarity of methodological strategies rather than the dominance of any single platform. Targeted LC–MS/MS and GC–MS(/MS) remain indispensable for robust quantification of priority contaminants and regulatory monitoring, whereas HRMS-based suspect and non-target screening has become essential for expanding chemical coverage and revealing overlooked contaminants, transformation products, and replacement compounds. In parallel, MP analysis requires integration of particle-resolved spectroscopic tools with complementary thermal and mass-based techniques, since no single platform currently provides full coverage across all relevant particle sizes, polymer classes, and environmental matrices.

Another key conclusion is that sampling design and sample preparation are not secondary methodological details, but fundamental determinants of analytical relevance. Event-triggered pulses, seasonal variability, first-flush effects, and precursor transformation can lead to substantial underestimation when monitoring relies only on sparse grab sampling. Likewise, matrix-adapted extraction and cleanup remain essential because salinity, dissolved organic matter, lipids, particulates, and co-extracted interferences strongly influence recoveries, matrix effects, and detection limits. Fit-for-purpose workflows tailored to water, sludge, sediment, soil, biota, and reuse systems are therefore necessary not only to improve sensitivity, but also to strengthen comparability and confidence in cross-study interpretation.

A distinctive contribution of this review is the integrated treatment of molecular and particulate emerging contaminants within a single analytical and risk-oriented framework. Rather than treating ECs and MPs as separate monitoring domains, the reviewed evidence highlights their convergence through shared occurrence in natural and treated waters, interactions during treatment and environmental transport, and combined implications for exposure under water-reuse and food-production scenarios. In this context, analytical undercoverage—including incomplete target lists, unresolved transformation products, the limited availability of commercially available standards, and methodological constraints in MP detection—remains a major factor limiting robust environmental and human-health risk assessment studies.

The evidence synthesized here further shows that apparent contaminant removal does not necessarily correspond to risk reduction. For molecular ECs, treatment can generate transformation products or redistribute contaminants between dissolved and particulate phases without eliminating hazard. For MPs, removal from the aqueous phase often reflects transfer to sludge and other solid compartments, creating secondary exposure pathways through biosolids reuse, wastewater irrigation, and terrestrial accumulation. This redistribution perspective is particularly important under increasing water scarcity and reuse, where contaminants may recirculate across connected water–soil–plant–food systems.

Overall, this review identifies four major priorities for the next generation of analytical frameworks: (i) harmonized and transparent sampling, QA/QC, and reporting practices across matrices and methods; (ii) systematic integration of targeted quantification with HRMS-enabled suspect and non-target screening for broader chemical coverage; (iii) combined particle-count, polymer-identity, and polymer-mass approaches for MPs and TWPs; and (iv) stronger coupling of analytical chemistry with toxicology, bioavailability assessment, and exposure modeling. Advancing these priorities will be essential to transform increasingly sophisticated analytical data into

 doi:10.20944/preprints202604.0384.v1

comparable, risk-relevant evidence and to support science-based decision-making on ECs and MPs in natural waters, wastewaters, reclaimed waters, and drinking-water-related systems.

Supplementary Materials: The following supporting information can be downloaded at the website of this paper posted on Preprints.org, Table S1. Comparative analytical strategies for molecular emerging contaminants in water and related matrices: instrumentation, analytical performance, identification capability, strengths, and limitations.

Author Contributions: Conceptualization, M.M. and D.B.; literature review, M.M.; data curation, M.M.; visualization, M.M.; writing—original draft preparation, M.M.; writing—review and editing, M.M. and D.B.; supervision, D.B. All authors have read and agreed to the published version of the manuscript.

Funding: This research received no external funding.

Institutional Review Board Statement: Not applicable.

Informed Consent Statement: Not applicable.

Data Availability Statement: No new data were created or analyzed in this study.

Acknowledgments: The authors gratefully acknowledge the support of their respective institutions.

Conflicts of Interest: The authors declare no conflict of interest.

References

1. Mallek, M.; Barceló, D. Assessment of Removal Technologies for Microplastics in Surface Waters and Wastewaters. *Curr. Opin. Chem. Eng.* **2025**, *49*, 101170.
2. Mallek, M.; Barceló, D. Advancing Water Treatment and Reuse Technologies to Address the Nexus of Climate Change, Water Scarcity, and Pharmaceutical Contamination. *J. Environ. Chem. Eng.* **2025**, *13*, 119284.
3. Li, X.; Shen, X.; Jiang, W.; Xi, Y.; Li, S. Comprehensive Review of Emerging Contaminants: Detection Technologies, Environmental Impact, and Management Strategies. *Ecotoxicol. Environ. Saf.* **2024**, *278*, 116420.
4. Chen, H.; Xie, J.; Huang, C.; Liang, Y.; Zhang, Y.; Zhao, X.; Ling, Y.; Wang, L.; Zheng, Q.; Yang, X. Database and Review of Disinfection By-Products since 1974: Constituent Elements, Molecular Weights, and Structures. *J. Hazard. Mater*. **2024**, *462*, 132792.
5. Mallek, M.; Barceló, D. Analysis and Fate of Per- and Polyfluoroalkyl Substances (PFAS) in the Global Aquatic Environment: Perspectives and Combined Risks with Microplastics. *Anal. Bioanal. Chem*. **2025**.
6. Du, J.; Xu, J.; Luo, Y.; Li, X.; Zhao, L.; Liu, S.; Jia, X.; Wang, Z.; Ge, L.; Cui, K.; et al. High-Throughput Monitoring of 323 Pharmaceuticals and Personal Care Products (PPCPs) and Pesticides in Surface Water for Environmental Risk Assessment. *Environ. Sci. Technol*. **2025**, *59*, 11275–11285.
7. Sahai, H.; Hernando, M.D.; Martínez Bueno, M.J.; Aguilera del Real, A.M.; Fernández-Alba, A.R. Evaluation of the Sorption/Desorption Processes of Pesticides in Biodegradable Mulch Films Used in Agriculture. *Chemosphere* **2024**, *351*, 141183.
8. Kazmi, S.S.U.H.; Xu, Q.; Tayyab, M.; Pastorino, P.; Barceló, D.; Yaseen, Z.M.; Khan, Z.H.; Li, G. Navigating the Environmental Dynamics, Toxicity to Aquatic Organisms and Human Associated Risks of an Emerging Tire Wear Contaminant 6PPD-Quinone. *Environ. Pollut*. **2024**, *356*, 124313.
9. Liao, C.; Kim, U. A Review of Environmental Occurrence, Fate, Exposure, and Toxicity of Benzothiazoles. *Environ. Sci. Technol*. **2018**, *52*, 5007–5026.
10. Rapp-Wright, H.; Rodríguez-Mozaz, S.; Alvarez-Muñoz, D.; Barceló, D.; Regan, F.; Barron, L.; White, B. International Comparison, Risk Assessment, and Prioritisation of 26 Endocrine Disrupting Compounds in Three European River Catchments in the UK, Ireland, and Spain. *Molecules* **2023**, *28*, 5994.
11. Jiang, C.; Liu, S.; Zhang, T.; Liu, Q.; Alvarez, P.; Chen, W. Current Methods and Prospects for Analysis and Characterization of Nanomaterials in the Environment. *Environ. Sci. Technol.* **2022**, *56*, 7426–7447.

 doi:10.20944/preprints202604.0384.v1

12. Dong, H.; Aziz, Md.T.; Richardson, S. Transformation of Algal Toxins during the Oxidation/Disinfection Processes of Drinking Water: From Structure to Toxicity. *Environ. Sci. Technol.* **2023**, *57*, 12944–12957.
13. Jaén-Gil, A.; Tisserand, A.; Santos, L.; Rodríguez-Mozaz, S.; Gomiero, A.; Langeland, E.; Khan, F. Legacy of Chemical Pollution from an Underwater Tire Dump in Alver Municipality, Norway: Implication for the Persistence of Tire-Derived Chemicals and Site Remediation. *Environments* **2025**, *12*, 356.
14. Qaiser, Z.; Aqeel, M.; Sarfraz, W.; Fatima Rizvi, Z.; Noman, A.; Naeem, S.; Khalid, N. Microplastics in Wastewaters and Their Potential Effects on Aquatic and Terrestrial Biota. *Case Stud. Chem. Environ. Eng.* **2023**, *8*, 100536.
15. González Fernández, D.; Cózar, A.; Hanke, G.; Viejo, J.; Morales-Caselles, C.; Bakiu, R.; Barceló, D.; Bessa, F.; Bruge, A.; Cabrera Fernández, M.; et al. Floating Macrolitter Leaked from Europe into the Ocean. *Nat. Sustain.* **2021**, *4*, 474–483.
16. Johannessen, C.; Helm, P.; Lashuk, B.; Yargeau, V.; Metcalfe, C.D. The Tire Wear Compounds 6PPD-Quinone and 1,3-Diphenylguanidine in an Urban Watershed. *Arch. Environ. Contam. Toxicol.* **2022**, *82*, 171–179.
17. WWF-Viet Nam. *Report on Plastic Waste Generation in 2022*; Thanh Nien Publishing House: Ha Noi, Viet Nam, **2023**.
18. Li, J.; Aziz, Md.T.; Granger, C.O.; Richardson, S.D. Halocyclopentadienes: An Emerging Class of Toxic DBPs in Chlor(Am)Inated Drinking Water. *Environ. Sci. Technol.* **2022**, *56*, 11387–11397.
19. Yu, L.; Lin, Y.; Li, J.; Deng, C.; Zhang, R.; Liu, A.; Wang, L.; Li, Y.; Wei, X.; Lu, D.; et al. Suspect Screening of Pharmaceuticals and Their Transformation Products (TPs) in Wastewater during COVID-19 Infection Peak: Identification of New TPs and Elevated Risks. *Environ. Sci. Technol.* **2025**, *59*, 4893–4905.
20. Wang, C.; Guo, R.; Guo, C.; Yin, H.; Xu, J. Photodegradation of Typical Psychotropic Drugs in the Aquatic Environment: A Critical Review. *Environ. Sci. Process. Impacts* **2025**, *27*, 320–354.
21. Boahen, E.; Owusu, L.; Adjei-Anim, S. A Comprehensive Review of Emerging Environmental Contaminants of Global Concern. *Discover Environment* **2025**, *3*, 144.
22. Ma, W.; Li, F.; Tian, Y.; Xu, H.; Luo, J.; Shi, D.; Dai, J.; Tang, J.; Pan, Y. Simultaneous Analysis of Ultrashort- to Long-Chain PFAS in Multisalinity Aquatic Systems: Methodology, Spatial Profiling, and Risk Prioritization. *Environ. Sci. Technol.* **2025**, *59*, 26770–26780.
23. Cao, G.; Wang, W.; Zhang, J.; Wu, P.; Qiao, H.; Li, H.; Huang, G.; Yang, Z.; Cai, Z. Occurrence and Fate of Substituted *p*-Phenylenediamine-Derived Quinones in Hong Kong Wastewater Treatment Plants. *Environ. Sci. Technol.* **2023**, *57*, 15635–15643.
24. Wang, X.; Yang, J.; Jiao, Z.; Liang, J.; Chen, Y.; Gao, Q.; Shi, W.; Zhang, X.; Yu, H.; Wei, S.; et al. Uncovering Overlooked Fluorinated Compounds by Multi-Strategy Nontarget Screening in an Urban River System in China. *Environ. Sci. Technol.* **2026**, *60*, 3567–3579.
25. Wang, W.; Cao, G.; Zhang, J.; Chang, W.; Sang, Y.; Cai, Z. Fragmentation Pattern-Based Screening Strategy Combining Diagnostic Ion and Neutral Loss Uncovered Novel *p*-Phenylenediamine Quinone Contaminants in the Environment. *Environ. Sci. Technol.* **2024**, *58*, 5921–5931.
26. Qian, Y.; Ke, Y.; Wang, L.; Yu, N.; He, Y.; Yu, Q.; Wei, S.; Ren, H.; Geng, J. Entropy Similarity-Driven Transformation Reaction Molecular Networking Reveals Transformation Pathways and Potential Risks of Emerging Contaminants in Wastewater: The Example of Sartans. *Environ. Sci. Technol.* **2025**, *59*, 4153–4164.
27. Lara-Martín, P.A.; Schinkel, L.; Eberhard, Y.; Giger, W.; Berg, M.; Hollender, J. Suspect and Nontarget Screening of Organic Micropollutants in Swiss Sewage Sludge: A Nationwide Survey. *Environ. Sci. Technol.* **2025**, *59*, 7688–7698.
28. Kumar, A.; Georgi, A.; Huaccallo-Aguilar, Y.; Meier, M.; Kryk, H.; Reinecke, S.F.; Hampel, U. Degradation and Defluorination of Perfluorooctane Sulfonate (PFOS) Forever Chemical in Water Using Hydrodynamic Cavitation Treatment. *Chem. Eng. J. Adv.* **2026**, *25*, 101046.
29. Mallek, M.; Barceló, D. Sustainable Analytical Approaches for Microplastics in Wastewater, Sludge, and Landfills: Challenges, Fate, and Green Chemistry Perspectives. *Adv. Sample Prep.* **2025**, *14*, 100178.
30. van Mourik, L.M.; Crum, S.; Martinez-Frances, E.; van Bavel, B.; Leslie, H.A.; de Boer, J.; Cofino, W.P. Results of WEPAL-QUASIMEME/NORMAN's First Global Interlaboratory Study on Microplastics Reveal Urgent Need for Harmonization. *Sci. Total Environ.* **2021**, *772*, 145071.

 doi:10.20944/preprints202604.0384.v1

31. Sumpter, J.P.; Runnalls, T.J.; Johnson, A.C.; Barceló, D. A 'Limitations' Section Should Be Mandatory in All Scientific Papers. *Sci. Total Environ.* **2023**, *857*, 159395.
32. Boisseaux, P.; Delignette-Muller, M.L.; Galloway, T. A Quantitative Environmental Risk Assessment for Microplastics in Sewage Sludge Applied to Land. *Environ. Sci. Technol.* **2025**, *59*, 26526–26538.
33. Hayes, A.; Zhang, L.; Snape, J.; Feil, E.; Kasprzyk-Hordern, B.; Gaze, W.H.; Murray, A.K. Common Non-Antibiotic Drugs Enhance Selection for Antimicrobial Resistance in Mixture with Ciprofloxacin. *ISME Commun.* **2025**, *5*, ycaf169.
34. Liu, X.; Wei, W.; Chen, Z.; Wu, L.; Duan, H.; Zheng, M.; Wang, D.; Ni, B.-J. The Threats of Micro- and Nanoplastics to Aquatic Ecosystems and Water Health. *Nat. Water* **2025**, 3, 764–781.
35. Pestana, C.J.; Moura, D.S.; Capelo-Neto, J.; Edwards, C.; Dreisbach, D.; Spengler, B.; Lawton, L.A. Potentially Poisonous Plastic Particles: Microplastics as a Vector for Cyanobacterial Toxins Microcystin-LR and Microcystin-LF. *Environ. Sci. Technol.* **2021**, *55*, 15940–15949.
36. Valenzuela-Lázaro, J.M.; González-Pleiter, M.; Leganés, F.; Martínez Bueno, M.J.; Fernández-Alba, A.R.; Rosal, R.; Fernández-Piñas, F. The Role of Greenhouse Agricultural Plastic Waste as a Reservoir of Antibiotic Resistance Genes and Vector of Their Environmental Dissemination. *Environ. Chem. Ecotoxicol.* **2025**, *7*, 1545–1559.
37. Fu, Q.; Malchi, T.; Carter, L.J.; Li, H.; Gan, J.; Chefetz, B. Pharmaceutical and Personal Care Products: From Wastewater Treatment into Agro-Food Systems. *Environ. Sci. Technol.* **2019**, *53*, 14083–14090.
38. Andreasidou, E.; Kovačič, A.; Manzano-Sánchez, L.; Heath, D.; Kosjek, T.; Pintar, M.; Maršič, N.K.; Blaznik, U.; Fernández-Alba, A.R.; Hernando, M.D.; et al. Uptake of Emerging Contaminants in Tomato Plants: A Field Study on Treated Wastewater Reuse. *Environ. Int.* **2025**, *205*, 109916.
39. Sanchís, J.; Jiménez-Lamana, J.; Abad, E.; Szpunar, J.; Farré, M. Occurrence of Cerium-, Titanium-, and Silver-Bearing Nanoparticles in the Besòs and Ebro Rivers. *Environ. Sci. Technol.* **2020**, *54*, 3969–3978.
40. Zheng, Z.; Zhang, R.; Hong, W.; Yang, S.; Lin, X.; Shu, W.; Price, G.W.; Song, L. Landfills as Hotspots of Multidrug Resistance Genes: Profiles, Drivers, and Hosts. *Environ. Sci. Technol.* **2025**, *59*, 25724–25737.
41. Yu, X.; Sui, Q.; Lyu, S.; Zhao, W.; Liu, J.; Cai, Z.; Yu, G.; Barceló, D. Municipal Solid Waste Landfills: An Underestimated Source of Pharmaceutical and Personal Care Products in the Water Environment. *Environ. Sci. Technol.* **2020**, *54*, 9757–9768.
42. Andrews, W.J.; Masoner, J.R.; Cozzarelli, I.M. Emerging Contaminants at a Closed and an Operating Landfill in Oklahoma. *Groundw. Monit. Remediat.* **2012**, *32*, 120–130.
43. Yu, X.; Sui, Q.; Lyu, S.; Zhao, W.; Wu, D.; Yu, G.; Barceló, D. Rainfall Influences Occurrence of Pharmaceutical and Personal Care Products in Landfill Leachates: Evidence from Seasonal Variations and Extreme Rainfall Episodes. *Environ. Sci. Technol.* **2021**, *55*, 4822–4830.
44. Ehalt Macedo, H.; Lehner, B.; Nicell, J.A.; Khan, U.; Klein, E.Y. Antibiotics in the Global River System Arising from Human Consumption. *PNAS Nexus* **2025**, *4*, pgaf096.
45. Wang, X.; Wang, Y.; Zhang, Z.; Tian, L.; Zhu, T.; Zhao, Y.; Tong, Y.; Yang, Y.; Sun, P.; Liu, Y. Effect, Fate and Remediation of Pharmaceuticals and Personal Care Products (PPCPs) during Anaerobic Sludge Treatment: A Review. *Environ. Sci. Technol.* **2024**, *58*, 19095–19114.
46. Ashfaq, M.; Li, Y.; Wang, Y.; Chen, W.; Wang, H.; Chen, X.; Wu, W.; Huang, Z.; Yu, C.-P.; Sun, Q. Occurrence, Fate, and Mass Balance of Different Classes of Pharmaceuticals and Personal Care Products in an Anaerobic-Anoxic-Oxic Wastewater Treatment Plant in Xiamen, China. *Water Res.* **2017**, *123*, 655–667.
47. Narumiya, M.; Nakada, N.; Yamashita, N.; Tanaka, H. Phase Distribution and Removal of Pharmaceuticals and Personal Care Products during Anaerobic Sludge Digestion. *J. Hazard. Mater.* **2013**, *260*, 305–312.
48. Zhang, H.; Yin, M.; Li, S.; Zhang, S.; Han, G. The Removal of Erythromycin and Its Effects on Anaerobic Fermentation. *Int. J. Environ. Res. Public Health* **2022**, *19*, 7256.
49. Xiang, Y.; Xiong, W.; Yang, Z.; Xu, R.; Zhang, Y.; Wu, M.; Ye, Y.; Peng, H.; Sun, W.; Wang, D. Metagenomic Insights into the Toxicity of Carbamazepine to Functional Microorganisms in Sludge Anaerobic Digestion. *Sci. Total Environ.* **2024**, *919*, 170780.
50. Li, Y.; Sallach, J.B.; Zhang, W.; Boyd, S.A.; Li, H. Characterization of Plant Accumulation of Pharmaceuticals from Soils with Their Concentration in Soil Pore Water. *Environ. Sci. Technol.* **2022**, *56*, 9346–9355.

 doi:10.20944/preprints202604.0384.v1

51. Kah, M.; Wilson, S.C.; Carter, L. The Fundamental Role of Healthy Soil in Maintaining Water Quality. *Nat. Water* **2025**, *3*, 1365–1375.
52. Molins-Delgado, D.; Díaz-Cruz, M.S.; Barceló, D. Introduction: Personal Care Products in the Aquatic Environment. In *Personal Care Products in the Aquatic Environment*; Díaz-Cruz, M.S., Barceló, D., Eds.; Springer International Publishing: Cham, Switzerland, **2015**; pp. 1–34.
53. Sang, Z.; Jiang, Y.; Tsoi, Y.-K.; Leung, K.S.-Y. Evaluating the Environmental Impact of Artificial Sweeteners: A Study of Their Distributions, Photodegradation and Toxicities. *Water Res.* **2014**, *52*, 260–274.
54. Pastorino, P.; Barceló, D.; Prearo, M. Alps at Risk: High-Mountain Lakes as Reservoirs of Persistent and Emerging Contaminants. *J. Contam. Hydrol.* **2024**, *264*, 104361.
55. Sanchís, J.; Berrojalbiz, N.; Caballero, G.; Dachs, J.; Farré, M.; Barceló, D. Occurrence of Aerosol-Bound Fullerenes in the Mediterranean Sea Atmosphere. *Environ. Sci. Technol.* **2012**, *46*, 1335–1343.
56. Yuan, B.; Letcher, R.J. Evolving Accumulation of a Complex Profile of Polychlorinated Alkanes in Canadian Polar Bears. *Environ. Sci. Technol. Lett.* **2024**, *11*, 591–597.
57. Elidrissi El Yallouli, N.; Lahrouni, M.; Mugani, R.; Oudra, B.; Poté, J. Insight in Limited Research on Environmental Factors and Health Implications of Toxic Cyanobacteria Bloom in African Freshwater Bodies. *Discover Public Health* **2024**, *21*, 202.
58. Marques dos Santos, M.; Snyder, S.A. Occurrence of Polymer Additives 1,3-Diphenylguanidine (DPG), *N*-(1,3-Dimethylbutyl)-*N*′-Phenyl-1,4-Benzenediamine (6PPD), and Chlorinated Byproducts in Drinking Water: Contribution from Plumbing Polymer Materials. *Environ. Sci. Technol. Lett.* **2023**, *10*, 885–890.
59. Seiwert, B.; Nihemaiti, M.; Troussier, M.; Weyrauch, S.; Reemtsma, T. Abiotic Oxidative Transformation of 6PPD and 6PPD-Quinone from Tires and Occurrence of Their Products in Snow from Urban Roads and in Municipal Wastewater. *Water Res.* **2022**, *212*, 118122.
60. Richardson, S.D.; Manasfi, T. Water Analysis: Emerging Contaminants and Current Issues. *Anal. Chem.* **2024**, *96*, 8184–8219.
61. Zhao, H.N.; Hu, X.; Gonzalez, M.; Rideout, C.A.; Hobby, G.C.; Fisher, M.F.; McCormick, C.J.; Dodd, M.C.; Kim, K.E.; Tian, Z.; et al. Screening *p*-Phenylenediamine Antioxidants, Their Transformation Products, and Industrial Chemical Additives in Crumb Rubber and Elastomeric Consumer Products. *Environ. Sci. Technol.* **2023**, *57*, 2779–2791.
62. Reddy, C.M.; Quinn, J.G. Environmental Chemistry of Benzothiazoles Derived from Rubber. *Environ. Sci. Technol.* **1997**, *31*, 2847–2853.
63. Ni, H.-G.; Lu, F.-H.; Luo, X.-L.; Tian, H.-Y.; Zeng, E.Y. Occurrence, Phase Distribution, and Mass Loadings of Benzothiazoles in Riverine Runoff of the Pearl River Delta, China. *Environ. Sci. Technol.* **2008**, *42*, 1892–1897.
64. Franklin, E.B.; Alves, M.R.; Moore, A.N.; Kilgour, D.B.; Novak, G.A.; Mayer, K.; Sauer, J.S.; Weber, R.J.; Dang, D.; Winter, M.; et al. Atmospheric Benzothiazoles in a Coastal Marine Environment. *Environ. Sci. Technol.* **2021**, *55*, 15705–15714.
65. Zhang, S.; Dai, Z.; Tang, Z.; Zhu, G.; Liu, W.; Zhang, C.; Li, J.; Yang, Y.; Yu, Z.; Lin, B.; et al. Workplace Presence and Exposure of *p*-Phenylenediamines and Their Quinones in Rubber Production. *Environ. Sci. Technol. Lett.* **2025**, *12*, 1418–1425.
66. Chen, X.; He, T.; Yang, X.; Gan, Y.; Qing, X.; Wang, J.; Huang, Y. Analysis, Environmental Occurrence, Fate and Potential Toxicity of Tire Wear Compounds 6PPD and 6PPD-Quinone. *J. Hazard. Mater.* **2023**, *452*, 131245.
67. Hu, X.; Zhao, H.N.; Tian, Z.; Peter, K.T.; Dodd, M.C.; Kolodziej, E.P. Chemical Characteristics, Leaching, and Stability of the Ubiquitous Tire Rubber-Derived Toxicant 6PPD-Quinone. *Environ. Sci. Process. Impacts* **2023**, *25*, 901–911.
68. Zoroufchi Benis, K.; Behnami, A.; Minaei, S.; Brinkmann, M.; McPhedran, K.N.; Soltan, J. Environmental Occurrence and Toxicity of 6PPD Quinone, an Emerging Tire Rubber-Derived Chemical: A Review. *Environ. Sci. Technol. Lett.* **2023**, *10*, 815–823.
69. Li, C.; Yang, Y.; Tian, Z.; Huang, Z.; Huang, Y.; Hong, Y. Residues of 6PPD-Q in the Aquatic Environment and Toxicity to Aquatic Organisms: A Review. *Fishes* **2025**, *10*, 146.

 doi:10.20944/preprints202604.0384.v1

70. Zhao, H.N.; Peter, K.T.; Gonzalez, M.; Rideout, C.A.; Hu, X.; Tian, Z.; Kolodziej, E.P. Temporal Dynamics of PPD-Class Antioxidants and Transformation Products in a Small Roadway-Runoff-Impacted Watershed. *Environ. Sci. Technol.* **2025**, *59*, 18358–18371.
71. Steinhoff, B.; Müller, J.; Mozhayeva, D.; Spelz, B.T.F.; Engelhard, C.; Butz, B.; Schönherr, H. Investigation of the Fate of Silver and Titanium Dioxide Nanoparticles in Model Wastewater Effluents via Selected Area Electron Diffraction. *Environ. Sci. Technol.* **2020**, *54*, 8681–8689.
72. Ma, R.; Levard, C.; Judy, J.D.; Unrine, J.M.; Durenkamp, M.; Martin, B.; Jefferson, B.; Lowry, G.V. Fate of Zinc Oxide and Silver Nanoparticles in a Pilot Wastewater Treatment Plant and in Processed Biosolids. *Environ. Sci. Technol.* **2014**, *48*, 104–112.
73. Stegemeier, J.P.; Avellan, A.; Lowry, G.V. Effect of Initial Speciation of Copper- and Silver-Based Nanoparticles on Their Long-Term Fate and Phytoavailability in Freshwater Wetland Mesocosms. *Environ. Sci. Technol.* **2017**, *51*, 12114–12122.
74. Lowry, G.V.; Espinasse, B.P.; Badireddy, A.R.; Richardson, C.J.; Reinsch, B.C.; Bryant, L.D.; Bone, A.J.; Deonarine, A.; Chae, S.; Therezien, M.; et al. Long-Term Transformation and Fate of Manufactured Ag Nanoparticles in a Simulated Large Scale Freshwater Emergent Wetland. *Environ. Sci. Technol.* **2012**, *46*, 7027–7036.
75. Windler, L.; Lorenz, C.; von Goetz, N.; Hungerbühler, K.; Amberg, M.; Heuberger, M.; Nowack, B. Release of Titanium Dioxide from Textiles during Washing. *Environ. Sci. Technol.* **2012**, *46*, 8181–8188.
76. Weir, A.; Westerhoff, P.; Fabricius, L.; Hristovski, K.; von Goetz, N. Titanium Dioxide Nanoparticles in Food and Personal Care Products. *Environ. Sci. Technol.* **2012**, *46*, 2242–2250.
77. Gondikas, A.P.; von der Kammer, F.; Reed, R.B.; Wagner, S.; Ranville, J.F.; Hofmann, T. Release of TiO2 Nanoparticles from Sunscreens into Surface Waters: A One-Year Survey at the Old Danube Recreational Lake. *Environ. Sci. Technol.* **2014**, *48*, 5415–5422.
78. Verwold, C.; Tremblay, C.; Patron, M.; Kimura, S. Total Organic Halogen (TOX) in Treated Wastewaters: Method Development and Comparison with Target Analysis; **2023**.
79. Zhou, X.; Zhao, X.; Chen, T.; Lv, J.; Guo, J.; Song, B.; Li, J.; Wang, Y.; Jiang, G. Comprehensive Assessment of Poly- and Perfluoroalkyl Substances in China: Flows, Stocks, and Emissions from Polytetrafluoroethylene. *Environ. Sci. Technol.* **2026**, *60*, 3886–3898.
80. Thompson, K.A.; Mortazavian, S.; Gonzalez, D.J.; Bott, C.; Hooper, J.; Schaefer, C.E.; Dickenson, E.R.V. Poly- and Perfluoroalkyl Substances in Municipal Wastewater Treatment Plants in the United States: Seasonal Patterns and Meta-Analysis of Long-Term Trends and Average Concentrations. *ACS ES&T Water* **2022**, *2*, 690–700.
81. Baqar, M.; Zhao, M.; Saleem, R.; Cheng, Z.; Fang, B.; Dong, X.; Chen, H.; Yao, Y.; Sun, H. Identification of Emerging Per- and Polyfluoroalkyl Substances (PFAS) in E-Waste Recycling Practices and New Precursors for Trifluoroacetic Acid. *Environ. Sci. Technol.* **2024**, *58*, 16153–16163.
82. Kudzin, G.P.; Dodds, J.N.; Kirkwood-Donelson, K.I.; Schiffenbauer, A.; Sarkar, K.; Noroozi Farhadi, P.; Miller, F.W.; Johnson, D.; Chappel, J.; Jarmusch, A.K.; et al. Evaluating Legacy and Emerging PFAS in Human Blood Collected from 2003 to 2021. *Environ. Sci. Technol.* **2026**, *60*, 3068–3079.
83. Teymoorian, T.; Delon, L.; Munoz, G.; Sauvé, S. Target and Suspect Screening Reveal PFAS Exceeding European Union Guideline in Various Water Sources South of Lyon, France. *Environ. Sci. Technol. Lett.* **2025**, *12*, 327–333.
84. Llamas, M.I.; Fernández-Valenzuela, P.J.; Vadillo, I.; Sanmiguel-Martí, M.; Rambla-Nebot, J.; Aranda-Mares, J.L.; Jiménez-Gavilán, P. Study of the Presence and Environmental Risk of Organic Contaminants Policed by the European Union and Other Organic Compounds in the Water Resources of a Region Overlapping Protected Areas: The Guadiaro River Basin (Southern Spain). *J. Environ. Manage.* **2023**, *345*, 118903.
85. Liu, N.; Jin, X.; Johnson, A.C.; Zhou, S.; Liu, Y.; Hou, L.; Meng, F.; Wu, F. Pharmaceutical and Personal Care Products (PPCPs) in Global Surface Waters: Risk and Drivers. *Environ. Sci. Technol.* **2025**, *59*, 19146–19159.
86. Guo, X.; Lv, M.; Song, L.; Ding, J.; Man, M.; Fu, L.; Song, Z.; Li, B.; Chen, L. Occurrence, Distribution, and Trophic Transfer of Pharmaceuticals and Personal Care Products in the Bohai Sea. *Environ. Sci. Technol.* **2023**, *57*, 21823–21834.

 doi:10.20944/preprints202604.0384.v1

87. Schildroth, S.; Bethea, T.N.; Wesselink, A.K.; Friedman, A.; Fruh, V.; Calafat, A.M.; Wegienka, G.; Gaston, S.; Baird, D.D.; Wise, L.A.; et al. Personal Care Products, Socioeconomic Status, and Endocrine-Disrupting Chemical Mixtures in Black Women. *Environ. Sci. Technol.* **2024**, *58*, 3641–3653.
88. Subedi, B.; Du, B.; Chambliss, C.K.; Koschorreck, J.; Rüdel, H.; Quack, M.; Brooks, B.W.; Usenko, S. Occurrence of Pharmaceuticals and Personal Care Products in German Fish Tissue: A National Study. *Environ. Sci. Technol.* **2012**, *46*, 9047–9054.
89. Bexfield, L.M.; Toccalino, P.L.; Belitz, K.; Foreman, W.T.; Furlong, E.T. Hormones and Pharmaceuticals in Groundwater Used as a Source of Drinking Water Across the United States. *Environ. Sci. Technol.* **2019**, *53*, 2950–2960.
90. Ziajahromi, S.; Lu, H.-C.; Drapper, D.; Hornbuckle, A.; Leusch, F.D.L. Microplastics and Tire Wear Particles in Urban Stormwater: Abundance, Characteristics, and Potential Mitigation Strategies. *Environ. Sci. Technol.* **2023**, *57*, 12829–12837.
91. Rauert, C.; Charlton, N.; Okoffo, E.D.; Stanton, R.S.; Agua, A.R.; Pirrung, M.C.; Thomas, K.V. Concentrations of Tire Additive Chemicals and Tire Road Wear Particles in an Australian Urban Tributary. *Environ. Sci. Technol.* **2022**, *56*, 2421–2431.
92. Cao, X.; Yue, T.; Meng, W.; Zhang, Y.; Li, J.; Yang, Y.; Su, G. Nontargeted Screening Unveils Structural Diversity and Environmental Pervasiveness of *p*-Phenylenediamine Antioxidant-Derived Quinones: Evidence from End-of-Life Tires and Road Dust Contamination. *Environ. Sci. Technol.* **2025**, *59*, 20630–20641.
93. Miller, S.A.; Schmidt, T.S.; Barber, L.B.; Hladik, M.L.; Kolpin, D.W.; Shoda, M.E.; Stackpoole, S.M. Imidacloprid in United States Rivers, 2013–2022: Persistent Presence and Emerging Chronic Hazard. *Environ. Sci. Technol.* **2025**, *59*, 26702–26715.
94. Hohrenk-Danzouma, L.L.; Vosough, M.; Merkus, V.I.; Drees, F.; Schmidt, T.C. Non-Target Analysis and Chemometric Evaluation of a Passive Sampler Monitoring of Small Streams. *Environ. Sci. Technol.* **2022**, *56*, 5466–5477.
95. León-Morán, L.O.; Pastor-Belda, M.; Viñas, P.; Arroyo-Manzanares, N.; Sánchez-Fernández, O.; Pérez-Ruzafa, Á.; Campillo, N. Targeted and Untargeted Approaches Using Liquid Chromatography with High-Resolution Mass Spectrometry for the Determination of Lipophilic Marine Biotoxins in Seawater and Mussel Samples. *Mar. Pollut. Bull.* **2026**, *222*, 118688.
96. Méndez, S.; Montes, R.; Raimundo, J.; López-Castillo, D.; López-Vázquez, J.; Caetano, M.; Lopes, C.; Figueiredo, C.; Pinheiro, M.; Alves, N.; et al. Screening of Organic Pollutants in Mollusc and Fish Samples from the Portuguese Coast by Combining Liquid and Gas Chromatography with High Resolution Mass Spectrometry. *Mar. Pollut. Bull.* **2026**, *222*, 118598.
97. *The Handbook of Environmental Chemistry*; Barceló, D., Kostianoy, A.G., Eds.; Springer: Cham, Switzerland, **2015**; Vol. 36.
98. Yu, X.; Zhao, W.; Lyu, S.; Cai, Z.; Yu, G.; Wang, H.; Barceló, D.; Sui, Q. Estimating the Mass of Pharmaceuticals Harbored in Municipal Solid Waste Landfills by Analyzing Refuse Samples at Various Ages and Depths. *Environ. Sci. Technol.* **2023**, *57*, 6063–6071.
99. Mehrabi, K.; Nowack, B.; Arroyo Rojas Dasilva, Y.; Mitrano, D.M. Improvements in Nanoparticle Tracking Analysis To Measure Particle Aggregation and Mass Distribution: A Case Study on Engineered Nanomaterial Stability in Incineration Landfill Leachates. *Environ. Sci. Technol.* **2017**, *51*, 5611–5621.
100. Pettibone, J.M.; Liu, J. In Situ Methods for Monitoring Silver Nanoparticle Sulfidation in Simulated Waters. *Environ. Sci. Technol.* **2016**, *50*, 11145–11153.
101. Smalling, K.L.; Romanok, K.M.; Bradley, P.M.; Morriss, M.C.; Gray, J.L.; Kanagy, L.K.; Gordon, S.E.; Williams, B.M.; Breitmeyer, S.E.; Jones, D.K.; et al. Per- and Polyfluoroalkyl Substances (PFAS) in United States Tapwater: Comparison of Underserved Private-Well and Public-Supply Exposures and Associated Health Implications. *Environ. Int.* **2023**, *178*, 108033.
102. Wicks, A.; Brady, S.; Whitehead, H.D.; Hedman, T.; Zachritz, A.; Venier, M.; Peaslee, G.F. Per- and Polyfluoroalkyl Substances in Reusable Feminine Hygiene Products. *Environ. Sci. Technol. Lett.* **2025**, *12*, 924–929.

 doi:10.20944/preprints202604.0384.v1

103. Xu, Y.; Ou, Q.; Wang, X.; Hou, F.; Li, P.; van der Hoek, J.P.; Liu, G. Assessing the Mass Concentration of Microplastics and Nanoplastics in Wastewater Treatment Plants by Pyrolysis Gas Chromatography–Mass Spectrometry. *Environ. Sci. Technol.* **2023**, *57*, 3114–3123.
104. Yang, T.; Luo, J.; Nowack, B. Characterization of Nanoplastics, Fibrils, and Microplastics Released during Washing and Abrasion of Polyester Textiles. *Environ. Sci. Technol.* **2021**, *55*, 15873–15881.
105. Paterson, K.; Beckingham, B.; Momplaisir, G.-M.; Varner, K. Adapting Methods for Isolation and Enumeration of Microplastics to Quantify Tire Road Wear Particles with Confirmation by Pyrolysis GC–MS. *Environ. Sci. Technol.* **2025**, *59*, 1769–1779.
106. Regan, F.; Allen, C.; Lawler, J. Demonstrating the Application of a Liquid Chromatography-Mass Spectrometry Method for the Determination of Phthalate Diesters in Complex Solid and Liquid Environmental Samples. *Anal. Methods* **2025**, 17, 8877–8888.
107. Kazmi, S.S.U.H.; Xu, Q.; Saqib, H.S.A.; Azeem, M.; Pastorino, P.; Barceló, D.; Yang, Q.; Li, G. Pollutant-Driven Humification of Dissolved Organic Matter Fails to Mitigate the Chronic Toxicity of Tire-Wear Contaminants in Freshwater Bioindicator. *Chem. Eng. J.* **2026**, *529*, 173274.
108. Gu, Y.; Feuerstein, M.L.; Lloyd, D.T.; Patel, C.J.; Johnson, C.H.; Warth, B. Quantitative Exposomics Targeting over 200 Toxicants and Key Biomarkers at the Picomolar Level. *Environ. Sci. Technol.* **2025**, *59*, 21818–21829.
109. Miller, T.R.; Xiong, A.; Deeds, J.R.; Stutts, W.L.; Samdal, I.A.; Løvberg, K.E.; Miles, C.O. Microcystin Toxins at Potentially Hazardous Levels in Algal Dietary Supplements Revealed by a Combination of Bioassay, Immunoassay, and Mass Spectrometric Methods. *J. Agric. Food Chem.* **2020**, *68*, 8016–8025.
110. Mahony, A.K.; Clair, T.A.; Mendez, M.A.; McNamara, P.J.; Arnold, W.A. Quaternary Ammonium Compounds in Wastewater Influents, Effluents, and Biosolids: Analysis from Twelve Wastewater Treatment Plants from 2020 to 2023. *Environ. Sci. Technol.* **2025**, *59*, 27929–27942.
111. Mills, C.; Dillon, M.J.; Kulabhusan, P.K.; Senovilla-Herrero, D.; Campbell, K. Multiplex Lateral Flow Assay and the Sample Preparation Method for the Simultaneous Detection of Three Marine Toxins. *Environ. Sci. Technol.* **2022**, *56*, 12210–12217.
112. Zhang, W.; Dixon, M.B.; Saint, C.; Teng, K.S.; Furumai, H. Electrochemical Biosensing of Algal Toxins in Water: The Current State-of-the-Art. *ACS Sens.* **2018**, *3*, 1233–1245.
113. Chow, C.-H.; Law, C.F.J.; Leung, K. Degradation of Acesulfame in UV/Monochloramine Process: Kinetics, Transformation Pathways and Toxicity Assessment. *J. Hazard. Mater.* **2021**, *403*, 123935.
114. Peng, W.; Law, J.C.-F.; Leung, K.S.-Y. Chlorination of Bisphenols in Water: Understanding the Kinetics and Formation Mechanism of 2-Butene-1,4-Dial and Analogues. *J. Hazard. Mater.* **2023**, *459*, 132128.
115. Hofstetter, T.B.; Bakkour, R.; Buchner, D.; Eisenmann, H.; Fischer, A.; Gehre, M.; Haderlein, S.B.; Höhener, P.; Hunkeler, D.; Imfeld, G.; et al. Perspectives of Compound-Specific Isotope Analysis of Organic Contaminants for Assessing Environmental Fate and Managing Chemical Pollution. *Nat. Water* **2024**, *2*, 14–30.
116. Boatman, A.K.; Chappel, J.R.; Kirkwood-Donelson, K.I.; Fleming, J.F.; Reif, D.M.; Schymanski, E.L.; Rager, J.E.; Baker, E.S. Updated Guidance for Communicating PFAS Identification Confidence with Ion Mobility Spectrometry. *Environ. Sci. Technol.* **2025**, *59*, 17711–17721.
117. Shafique, I.; Ahmad, R.; Shin, K.-H.; Cho, Y.; Oh, N.-H.; Hur, J.; Kim, S. Uncovering Hidden Pollution: Diffuse Contaminant Sources in a Sparsely Industrialized Estuarine System. *ACS ES&T Water* **2025**, *5*, 6994–7004.
118. Yao, J.; Sheng, N.; Guo, Y.; Yeung, L.W.Y.; Dai, J.; Pan, Y. Nontargeted Identification and Temporal Trends of Per- and Polyfluoroalkyl Substances in a Fluorochemical Industrial Zone and Adjacent Taihu Lake. *Environ. Sci. Technol.* **2022**, *56*, 7986–7996.
119. Arp, H.P.H.; Gredelj, A.; Glüge, J.; Scheringer, M.; Cousins, I.T. The Global Threat from the Irreversible Accumulation of Trifluoroacetic Acid (TFA). *Environ. Sci. Technol.* **2024**, *58*, 19925–19935.
120. Celma, A.; Sancho, J.V.; Schymanski, E.L.; Fabregat-Safont, D.; Ibáñez, M.; Goshawk, J.; Barknowitz, G.; Hernández, F.; Bijlsma, L. Improving Target and Suspect Screening High-Resolution Mass Spectrometry Workflows in Environmental Analysis by Ion Mobility Separation. *Environ. Sci. Technol.* **2020**, *54*, 15120–15131.

 doi:10.20944/preprints202604.0384.v1

121. Luo, Y.-S.; Aly, N.; McCord, J.; Strynar, M.; Chiu, W.; Dodds, J.; Baker, E.; Rusyn, I. Rapid Characterization of Emerging Per- and Polyfluoroalkyl Substances in Aqueous Film-Forming Foams Using Ion Mobility Spectrometry–Mass Spectrometry. *Environ. Sci. Technol.* **2020**, *54*, 15024–15034.
122. Camdzic, D.; Dickman, R.A.; Joyce, A.S.; Wallace, J.S.; Ferguson, P.L.; Aga, D.S. Quantitation of Total PFAS Including Trifluoroacetic Acid with Fluorine Nuclear Magnetic Resonance Spectroscopy. *Anal. Chem.* **2023**, *95*, 5484–5488.
123. Smolinski, R.; Koelmel, J.P.; Stelben, P.; Weil, D.; Godri, D.; Schiessel, D.; Kummer, M.; Stow, S.M.; Mohsin, S.; Royer, L.; et al. FluoroMatch IM: An Interactive Software for PFAS Analysis by Ion Mobility Spectrometry. *Environ. Sci. Technol.* **2025**, *59*, 6636–6648.
124. Motteau, S.; Dervilly, G.; Cariou, R.; Margalef, M.; Lamoree, M.; Hamers, T.; König, M.; Escher, B.I.; Vinggaard, A.M.; Rørbye, C.; et al. Determination of Chemical Mixtures in Environmental, Food, and Human Samples Using High-Resolution Mass Spectrometry-Based Suspect Screening Approaches. *Environ. Sci. Technol.* **2025**, *59*, 21265–21277.
125. Graves, L.G.; Zarfl, C.; Hirsch, T.; Vitale, G.A.; Petras, D.; Spahr, S. Target and Nontarget Analyses Reveal Similar Dissolved Organic Contaminant Patterns Relative to Quantified Catchment Characteristics along Two German Rivers. *Environ. Sci. Technol.* **2026**, *60*, 3580–3591.
126. Zou, Q.; Zhang, Q.; Yang, R.; Li, Y.; Pei, Z.; Liu, M.; Zhang, G.; Ji, F.; Zhang, X.; Yang, X.; et al. Non-Negligible Polyhalogenated Carbazoles in Arctic Soils and Sediments: Occurrence, Target and Suspect Screening, and Potential Sources. *Environ. Sci. Technol.* **2024**, *58*, 23169–23179.
127. Schymanski, E.L.; Jeon, J.; Gulde, R.; Fenner, K.; Ruff, M.; Singer, H.P.; Hollender, J. Identifying Small Molecules via High Resolution Mass Spectrometry: Communicating Confidence. *Environ. Sci. Technol.* **2014**, *48*, 2097–2098.
128. Nanusha, M.Y.; Frøkjær, E.E.; Søndergaard, J.; Mørk Larsen, M.; Schwartz Glottrup, C.; Bruun Nicolaisen, J.; Hansen, M. Quantitative Non-Targeted Screening to Profile Micropollutants in Sewage Sludge Used for Agricultural Field Amendments. *Environ. Sci. Technol.* **2024**, *58*, 9850–9862.
129. Sun, Y.; Zhou, Y.; Chen, Y.; Xie, Z.; Qiu, J.; Zhu, F.; Ouyang, G.; Yang, X. Stable Isotopic Labeling and Automated Reactivity-Directed Approach Accelerating Discovery of Toxic Disinfection Byproducts in Chlorinated and Chloraminated Waters. *Environ. Sci. Technol.* **2026**, *60*, 3486–3496.
130. Maurer, L.; Carmona, E.; Machate, O.; Schulze, T.; Krauss, M.; Brack, W. Contamination Pattern and Risk Assessment of Polar Compounds in Snow Melt: An Integrative Proxy of Road Runoffs. *Environ. Sci. Technol.* **2023**, *57*, 4143–4152.
131. Black, G.P.; Anderson, B.N.; Wong, L.; Alaimo, C.P.; He, G.; Denison, M.S.; Bennett, D.H.; Tancredi, D.; Durbin-Johnson, B.; Hammock, B.D.; et al. Comprehensive Nontargeted Analysis of Drinking Water Supplies to Identify Chemicals Associated with Estrogen Receptor Agonism or Present in Regions of Elevated Breast Cancer Occurrence. *Environ. Sci. Technol.* **2025**, *59*, 5237–5248.
132. Liu, X.; Xu, C.; Wu, J.; Foo, Y.H.; Zhou, J.; Wu, B.; Chan, L.L. Automatic MS/MS Data Mining Strategy for Rapid Screening of Polyether Toxins Derived from *Gambierdiscus* Species. *Anal. Chem.* **2025**, *97*, 5643–5652.
133. Li, Q.; Lai, Y.; Li, P.; Liu, X.; Yao, Z.; Liu, J.; Yu, S. Evaluating the Occurrence of Polystyrene Nanoparticles in Environmental Waters by Agglomeration with Alkylated Ferroferric Oxide Followed by Micropore Membrane Filtration Collection and Py-GC/MS Analysis. *Environ. Sci. Technol.* **2022**, *56*, 8255–8265.
134. Okoffo, E.D.; Chan, C.M.; Rauert, C.; Kaserzon, S.; Thomas, K.V. Identification and Quantification of Micro-Bioplastics in Environmental Samples by Pyrolysis–Gas Chromatography–Mass Spectrometry. *Environ. Sci. Technol.* **2022**, *56*, 13774–13785.
135. Li, P.; Lai, Y.; Zheng, R.; Li, Q.; Sheng, X.; Yu, S.; Hao, Z.; Cai, Y.; Liu, J. Extraction of Common Small Microplastics and Nanoplastics Embedded in Environmental Solid Matrices by Tetramethylammonium Hydroxide Digestion and Dichloromethane Dissolution for Py-GC-MS Determination. *Environ. Sci. Technol.* **2023**, *57*, 12010–12018.
136. Gahn, M.B.; Wharton, M.; Mortuza, A.; Hala, D.; Marshall, C.D.; Kaiser, K. Rapid and Sensitive Quantification of Nano- and Microplastics in Water, Sediment, and Biological Tissue by Pyrolysis-Gas Chromatography Tandem Mass Spectrometry with Dynamic Reaction Monitoring. *Anal. Chem.* **2026**, *98*, 633–641.

 doi:10.20944/preprints202604.0384.v1

137. Wang, Y.; Davis, I.; Shin, I.; Wherritt, D.J.; Griffith, W.P.; Dornevil, K.; Colabroy, K.L.; Liu, A. Biocatalytic Carbon–Hydrogen and Carbon–Fluorine Bond Cleavage through Hydroxylation Promoted by a Histidyl-Ligated Heme Enzyme. *ACS Catal.* **2019**, *9*, 4764–4776.
138. Dalmijn, J.; Glüge, J.; Scheringer, M.; Cousins, I.T. Emission Inventory of PFAS and Other Fluorinated Organic Substances for the Fluoropolymer Production Industry in Europe. *Environ. Sci. Process. Impacts* **2023**, *25*, 1806–1819.
139. Zhang, Y.; Guo, C.; Wu, R.; Hou, S.; Liu, Y.; Zhao, J.; Jiang, M.; Xu, J.; Wu, F. Global Occurrence, Distribution, and Ecological Risk Assessment of Psychopharmaceuticals and Illicit Drugs in Surface Water Environment: A Meta-Analysis. *Water Res.* **2024**, *263*, 122165.
140. Sanchís, J.; Olmos, M.; Vincent, P.; Farré, M.; Barceló, D. New Insights on the Influence of Organic Co-Contaminants on the Aquatic Toxicology of Carbon Nanomaterials. *Environ. Sci. Technol.* **2016**, *50*, 961–969.
141. Forster, A.L.B.; Wiskur, S.L.; Richardson, S.D. Formation of Eight Classes of DBPs from Chlorine, Chloramine, and Ozone: Mechanisms and Formation Pathways. *Environ. Sci. Technol.* **2025**, *59*, 15594–15611.
142. McIntyre, J.K.; Prat, J.; Cameron, J.; Wetzel, J.; Mudrock, E.; Peter, K.T.; Tian, Z.; Mackenzie, C.; Lundin, J.; Stark, J.D.; et al. Treading Water: Tire Wear Particle Leachate Recreates an Urban Runoff Mortality Syndrome in Coho but Not Chum Salmon. *Environ. Sci. Technol.* **2021**, *55*, 11767–11774.
143. Süßmuth, R.; Rosenberger, T.; Schweyen, P.; Dierkes, G.; Bell, A.M.; Wick, A.; Buchinger, S.; Ternes, T.A. Deciphering the Estrogenic Activity of Aqueous Leachates from Elastomers by Effect-Directed Analysis. *Environ. Sci. Technol.* **2025**, *59*, 21442–21453.
144. Zhang, Y.; Guo, C.; Sun, S.; Xie, M.; Wang, X.; Liu, S.; Xu, J.; Wu, F. Cigarette Filters—A Neglected Source of Phthalate Exposure to Humans. *Environ. Sci. Technol. Lett.* **2025**, *12*, 137–143.
145. Rodgers, T.F.M.; Drew, S.; Brown, T.; Hiki, K.; Hiroshi, Y.; King, M.; Kolodziej, E.P.; Krogh, E.T.; McIntyre, J.K.; Miller, K.; et al. Turning the Corner on Hazardous Tire Compounds: A Management Framework for Tire Additive Pollution. *Environ. Sci. Technol. Lett.* **2025**, *12*, 869–880.
146. Thomas, J.; Patil, R. The Road to Sustainable Tire Materials: Current State-of-the-Art and Future Prospectives. *Environ. Sci. Technol.* **2023**, *57*, 2209–2216.
147. Eckelman, M.J.; Mauter, M.S.; Isaacs, J.A.; Elimelech, M. New Perspectives on Nanomaterial Aquatic Ecotoxicity: Production Impacts Exceed Direct Exposure Impacts for Carbon Nanotubes. *Environ. Sci. Technol.* **2012**, *46*, 2902–2910.
148. Pu, Y.; Tang, F.; Adam, P.-M.; Laratte, B.; Ionescu, R.E. Fate and Characterization Factors of Nanoparticles in Seventeen Subcontinental Freshwaters: A Case Study on Copper Nanoparticles. *Environ. Sci. Technol.* **2016**, *50*, 9370–9379.
149. Conway, J.R.; Adeleye, A.S.; Gardea-Torresdey, J.; Keller, A.A. Aggregation, Dissolution, and Transformation of Copper Nanoparticles in Natural Waters. *Environ. Sci. Technol.* **2015**, *49*, 2749–2756.
150. Holden, P.A.; Gardea-Torresdey, J.L.; Klaessig, F.; Turco, R.F.; Mortimer, M.; Hund-Rinke, K.; Cohen Hubal, E.A.; Avery, D.; Barceló, D.; Behra, R.; et al. Considerations of Environmentally Relevant Test Conditions for Improved Evaluation of Ecological Hazards of Engineered Nanomaterials. *Environ. Sci. Technol.* **2016**, *50*, 6124–6145.
151. Dong, H.; Aziz, Md.T.; Richardson, S.D. Transformation of Algal Toxins during the Oxidation/Disinfection Processes of Drinking Water: From Structure to Toxicity. *Environ. Sci. Technol.* **2023**, *57*, 12944–12957.
152. Bei, E.; Li, X.; Wu, F.; Li, S.; He, X.; Wang, Y.; Qiu, Y.; Wang, Y.; Wang, C.; Wang, J.; et al. Formation of *N*-Nitrosodimethylamine Precursors through the Microbiological Metabolism of Nitrogenous Substrates in Water. *Water Res.* **2020**, *183*, 116055.
153. Agathokleous, E.; Peñuelas, J.; Azevedo, R.A.; Rillig, M.C.; Sun, H.; Calabrese, E.J. Low Levels of Contaminants Stimulate Harmful Algal Organisms and Enrich Their Toxins. *Environ. Sci. Technol.* **2022**, *56*, 11991–12002.
154. Shi, Y.; Xia, W.; Liu, H.; Liu, J.; Cao, S.; Fang, X.; Li, S.; Li, Y.; Chen, C.; Xu, S. Trihalomethanes in Global Drinking Water: Distributions, Risk Assessments, and Attributable Disease Burden of Bladder Cancer. *J. Hazard. Mater.* **2024**, *469*, 133760.

 doi:10.20944/preprints202604.0384.v1

155. Chen, R.; Zhou, Y.; Wang, Y.; Cheng, R.; Li, P.; Wang, Y.; Jiang, Y.; Wang, J.; Fu, Y.; Ni, B.; et al. Benzotriazoles and Benzothiazoles, Maternal and Neonatal Thyroid Hormones, and Childhood Growth: A Longitudinal Cohort Study. *Environ. Sci. Technol.* **2025**, *59*, 20967–20977.
156. Moulton, C.; Baroni, A.; Tasciotti, E. Micro- and Nanoplastics Exposure Across the Lifespan: One Health Implications for Aging and Longevity. *J. Xenobiot.* **2026**, *16*, 52.
157. Bayattork, M.; Rahman, M.; Hossain, M.I.; Zhang, Y.; Haque, A.N.M.A.; Kim, B.; Naebe, M. Impact of Textile-Derived Micro- and Nanoplastics on Brain Health: An Emerging Environmental Risk. *Environ. Sci. Technol.* **2026**, *60*, 2863–2895.
158. Šmídová, K.; Soinne, H.; Kim, S.W.; Tirronniemi, J.; Meffe, R.; Redondo-Hasselerharm, P.E.; Braun, M.; Rillig, M.C.; Fritze, H.; Adamczyk, B.; et al. Conventional and Biodegradable Agricultural Microplastics: Effects on Soil Properties and Microbial Functions across a European Pedoclimatic Gradient. *Environ. Pollut.* **2025**, 386, 127212.